01

Technical Report No. 42

SACLANT ASW
RESEARCH CENTRE

A DETAILED STUDY OF SOUND REFLECTIONS FROM A LAYERED OCEAN BOTTOM

by

P. STANGERUP

15 MAY 1965

NATO

VIALE SAN BARTOLOMEO, 92
LA SPEZIA, ITALY

This document is released to a NATO Government at the direction of the SACLANTCEN subject to the following conditions:

1. The recipient NATO Government agrees to use its best endeavours to ensure that the information herein disclosed, whether or not it bears a security classification, is not dealt with in any manner (a) contrary to the intent of the provisions of the Charter of the Centre, or (b) prejudicial to the rights of the owner thereof to obtain patent, copyright, or other like statutory protection therefor.

2. If the technical information was originally released to the Centre by a NATO Government subject to restrictions clearly marked on this document the recipient NATO Government agrees to use its best endeavours to abide by the terms of the restrictions so imposed by the releasing Government.

TECHNICAL REPORT NO. 42

SACLANT ASW RESEARCH CENTRE
Viale San Bartolomeo 92
La Spezia, Italy

A DETAILED STUDY OF SOUND REFLECTIONS FROM A LAYERED OCEAN BOTTOM

By

P. Stangerup

15 May, 1965

APPROVED FOR DISTRIBUTION

Henrik Nödtvedt
HENRIK NØDTVEDT
Director

TABLE OF CONTENTS

A DETAILED STUDY OF SOUND REFLECTIONS FROM A LAYERED OCEAN BOTTOM

By

P. Stangerup

ABSTRACT

The effect of layered sediments on sound reflection from the ocean bottom has been investigated theoretically and experimentally. Very detailed, systematic and computer-aided calculations of the reflection coefficient of a two-layer bottom are made, using well-known theory and varying the following parameters: (1) velocity and density contrasts; (2) layer thickness normalized with respect to wavelength; (3) absorption in the sediments (in db/wavelength); (4) shear wave velocity in the lower layer. Calculations are made both for a harmonic source and for a broadband source analysed within certain bands around the harmonic source frequency. A series of curves is obtained representing the two-layer effect for a range of parameters that encompasses typical ocean bottom values. It is shown that absorption in the upper layer is of great importance in sound reflection, especially beyond a critical angle, but that moderate shear wave velocities have little effect. An octave band analysis of experimental data — using a broadband source — tends to support this theoretical two-layer model.

INTRODUCTION

Very low frequency sound has long been used to investigate the characteristics of the oceans' deep bottom sediments and has often revealed distinct layers of different materials. However, it is only during the last few years that higher frequency sound has been used for similar studies of the layering in the upper tens of metres of the sediment. This has also aroused interest in attempts to explain the ocean-bottom sound-reflection mechanism for frequencies in the kilocycle region by using coring samples.

In fact, the sound reflection loss in the ocean bottom can seldom be explained by a model in which the bottom is considered as a simple, homogeneous, semi-infinite reflector. As short-pulse echo-soundings show, the higher bottom sediments often consist of a complicated system of thin, horizontal layers believed to be produced by turbidity currents, volcanic deposits, etc. Furthermore, the acoustic parameters of these sediments can depend on their age.

Many investigators (Refs. 1, 2 & 3) have tried to explain the bottom-reflection loss by multilayered reflectors consisting of two or more horizontal layers of different acoustic impedance. The present report describes a more systematic, theoretical survey of the subject. It will be shown that rather simple models can be used in many cases, because layers that are thin with respect to the wavelength of the sound have a very small effect and because high frequency sound might not penetrate through many layers because of absorption.

The presently described survey has therefore been carried out for a two-layer reflector in which the lower layer is semi-infinite and in which the thickness of the upper layer has been normalized with respect to the wavelength. Shearwaves in the lower layer and the effects of absorption have also been taken into account.

1. THEORY

1.1 Reflection Coefficient

The amplitude-reflection coefficient for the sea-bottom can, in the plane-wave case, be calculated in a simple way: -

$$R = \frac{Z_{in} - Z_w}{Z_{in} + Z_w}$$

where Z_w is the acoustic impedance of the water and Z_{in} is the acoustic input impedance of the bottom. This is completely analogous with the reflection from an impedance $Z_L = Z_{in}$ at the end of a transmission line of characteristic impedance $Z_o = Z_w$.

For vertical incidence the acoustic impedance of water is

$$Z_w = \rho_w C_w$$

where ρ_w is the density of the water and C_w is the sound velocity in it. The input impedance of the reflector is equal to the acoustic impedance of the reflecting medium, if the latter is semi-infinite. In transmission line theory this corresponds to having the input impedance equal to the characteristic impedance for an infinitely long line.

When the angle of incidence is different from zero, the velocity used in the expressions for the impedances should be the vertical phase velocity, which is

$$\frac{C}{\cos \theta}$$

where θ is the angle of incidence. This is illustrated in Fig. 1.

The angles of incidence in the water and the reflector are connected through Snell's law

$$k_w \sin \theta_w = k_B \sin \theta_B$$

where k_w and k_B are the wave numbers in water and reflector respectively ($k = \frac{2\pi f}{C}$, f being the frequency).

A layered reflector is analogous to a series connection of transmission lines of different characteristic impedances. The input impedance of a transmission line of length ℓ and characteristic impedance Z_o, loaded with an impedance Z_L, is known to be

$$Z_{in} = \frac{Z_L + i\, Z_o \tan\phi}{Z_o + i\, Z_L \tan\phi} \quad Z_o$$

where $\phi = \gamma\ell$ is the phase change along the line, γ being the phase shift per unit length.

An n-layered reflector is shown in Fig. 2, the layers being labelled from the lowest upwards. It is now easy to find the input impedance of the j^{th} layer because it can be expressed by the input impedance, $Z_{in}^{(j-1)}$, of the $(j-1)^{st}$

layer and the acoustical impedance, Z_j, of the j^{th} layer (Ref. 4).

$$Z_{in}^{(j)} = \frac{Z_{in}^{(j-1)} - i Z_j \tan \phi_j}{Z_j - i Z_{in}^{(j-1)} \tan \phi_j} Z_j$$

$$\phi_j = k_j h_j \cos \theta_j$$

where k_j is the wave number in the j^{th} layer

h_j is the thickness of the j^{th} layer, and

θ_j is the angle of incidence in the j^{th} layer.

By using this formula and the fact that the lowest layer is semi-infinite (i.e. $Z_{in}^{(1)} = Z_1$), it is now possible to find the input impedance of the whole system of layers seen from the water above. The reflection coefficient is then found from

$$R = \frac{Z_{in} - Z_w}{Z_{in} + Z_w}$$

The analogy with transmission lines shows that the problem of sound reflection can, in principle, be solved by means of a Smith chart (Ref. 5) — at least for angles of incidence smaller than the critical angle. However, the Smith chart will probably not be accurate enough and a computer should be used. As will be shown later, the computer programme turns out to be quite simple, even when absorption is present.

1.2 Introduction of absorption for n-layer bottoms

Bottom sediments are lossy media. It is therefore natural to include the effect of absorption in the calculations.

If absorption is absent, a plane sound wave can be characterized in the following way: -

$$\psi = A\, e^{-j(\omega t + kx)}$$

where k is the wave number. If absorption is present, a factor $e^{\alpha x}$ must be added, giving

$$\psi = A\, e^{\alpha x}\, e^{-j(\omega t + kx)}$$

$$= A\, e^{-j[\omega t + (k + j\alpha)x]}$$

$$= A\, e^{-j(\omega t + \gamma x)}$$

This means that the propagation constant is now complex and that Snell's law becomes

$$\gamma_w \sin \theta_w = \gamma_j \sin \theta_j$$

where $\gamma_w = k_w + j\alpha_w$ and $\gamma_j = k_j + j\alpha_j$

are the propagation constants in the water and in the j^{th} layer respectively. Thus the angle of incidence in the j^{th} layer becomes complex, namely

$$\sin \theta_j = \frac{k_w}{k_j + j\alpha_j} \sin \theta_w$$

if absorption in the water is ignored.

The real parts of the propagation constants determine the sound velocity in the various media

$$C_w = \frac{\omega}{k_w} \; ; \qquad C_j = \frac{\omega}{k_j} \quad \text{etc.},$$

while the imaginary parts, α_j, are the absorptions in Neper/unit length.

The impedances can now be defined as

$$Z_j = \frac{\rho_j \, \omega}{k + j\alpha}$$

for vertical incidence and

$$Z_j = \frac{\rho_j \, \omega}{(k + j\alpha) \cos \theta_j}$$

for oblique incidence,which reduces to $Z_j = \dfrac{\rho_j \, C_j}{\cos \theta_j}$ if absorption is absent.

1.3 Introduction of shearwaves in the lowest layer

The effect of shearwaves can easily be introduced if they exist only in the semi-infinite lowest layer, since this will only modify the impedance of this layer.

If shearwaves exist in other layers than the lowest, the problem becomes much more complicated and cannot be solved on a basis of impedance, since each reflection from a boundary between two media will give rise to both a compressional wave and a shearwave. In this case the problem must be solved using the boundary conditions for the potentials at each boundary, but this will not be treated in the present report.

It can be shown (Ref. 4) that the input impedance of a semi-infinite medium with shearwaves can be written

$$Z_{in} = Z_p \cos^2 2\theta_s + Z_s \sin^2 2\theta_s$$

where $Z_p = \dfrac{\rho\omega}{\gamma_p \cos\theta_p}$ and $Z_s = \dfrac{\rho\omega}{\gamma_s \cos\theta_s}$

and where γ_p and γ_s are the propagation constants (complex if absorption is present) for the compressional waves and the shearwaves respectively. θ_p and θ_s are related to the angle of incidence θ_w in the water through Snell's law

$$k_w \sin\theta_w = \gamma_p \sin\theta_p = \gamma_s \sin\theta_s$$

2. CALCULATED RESULTS

2.1 Effect of the upper layer thickness

On the basis of the above theories, a computer programme has been written to compute the reflection loss for a reflector consisting of an arbitrary number of layers. Absorption can be included in all the layers, and shearwaves can exist in the lowest layer.

The programme exists in two forms. One which computes the reflection loss when a harmonic sound source is used, and the other which computes the reflection loss for a broadband source analyzed in arbitrary frequency bands, taking into account the bandwidth of the filter and the spectrum of the sound source.

The programme has been used to calculate the effects of varying the thickness of the upper layer, the velocity contrasts and the absorption in a theoretical study of a two-layer bottom model.

In Figs. 3 and 4 are shown the reflection loss vs. angles of incidence for different values of the thickness of the upper layer when absorption is absent. Results are computed for two examples. In the first, the velocity of the upper layer is lower than the velocity in the water, while in the second the velocity of the upper layer is slightly higher than that in the water. The velocity in the lower layer is in both cases higher than in the upper layer and higher than the velocity in the water. These two examples are believed to represent two important cases of two-layered bottoms.

The curves for zero layer thickness show the reflection loss for the case in which only the lower medium exists. When the upper layer is thin in comparison with the wave length of the sound, the reflection loss will be very close to the reflection loss for the lower layer alone, because nearly all the energy leaks through such a thin layer.

When the upper layer becomes a quarter wave length thick, there is a relatively high loss at vertical incidence. This will always be the case when the lower layer has a higher impedance than the upper one. From transmission line theory it is known that a quarter wave length line will transform an impedance Z_L to an input impedance Z_{in}, which is

$$Z_{in} = \frac{Z_o^{\ 2}}{Z_L}$$

where Z_o is the characteristic impedance of the line. This means that the low impedance upper layer (the impedance of this is however higher than that of the water) will transform the high impedance of the lower layer into an impedance that is quite close to the impedance of the water. In other words, one is closer to an impedance-matching and more of the energy is transmitted into the bottom.

When the layer becomes half a wave length thick,the input impedance for vertical incidence is exactly the same as the impedance of the lower layer, i.e. the reflection loss is the same as if the upper layer does not exist. At about 60^o angle of incidence (exactly 60^o in the upper layer) the layer becomes a quarter wave length layer, since the vertical phase velocity in the upper layer becomes

$$\frac{C_{up}}{\cos \theta_{up}} = 2\ C_{up}$$

This means a minimum in the curve at this angle.

Beyond the critical angle for the lower layer (this angle is reached earlier than in the upper layer because of the higher velocity) the reflection becomes total. This can be explained by the fact that beyond a critical angle the input impedance of the medium is purely imaginary. This means that the input impedance of the whole system will also be purely imaginary, since a transmission line loaded by a pure reactance impedance will always show a purely reactive input impedance, independent of the length of the line.

As the layer becomes thicker than half a wave length, a series of maxima and minima will show up. The maxima will occur for angles of incidence for which the upper layer becomes half a wave length with respect to the vertical phase velocity. The upper envelope for the curve will be the reflection loss curve for a reflector consisting of only the lower semi-infinite medium. The minima will occur for angles of incidence at which the layer thickness with respect to the vertical phase velocity becomes an odd multiple of a quarter wave length.

2.2 Effects of absorption and of source bandwidth

Figures 5 to 16 have been drawn to show the effects of absorption on the reflection loss for different layer thicknesses. Each figure is divided into three columns. In the left-hand column are shown some of the same cases as described above but, in addition, showing the effect of absorption. In most cases the absorption in the sediments seems to diminish the oscillations of the reflection loss curves, but in a few cases the opposite occurs, especially for the thinner layers and around the critical angle. It is also seen that absorption in the lower layer has much less effect than that in the upper layer.

The middle column shows computed results, using a broad band white source through a filter 1/3 of an octave broad around the frequency for which the layer thickness is normalized.

The right-hand column shows the results using a broad band source in an octave band.

It is seen that the characteristic shape of the curves for a given layer thickness is the same in the 1/3 octave band when layer thicknesses are less than one wave length as it is for a harmonic source. For the octave bands this is only the case for layers thinner than half a wave length at the centre frequency of the band. At thicker layers all interesting effects are averaged out in the broad bands. If an explosive sound source is used, the analysis should not be made in broad frequency bands — which is often the case — but by a Fourier analysis.

However, by comparing the curves for the harmonic source with the curves for the octave band it is seen that phenomena beyond the critical angles are relatively frequency-independent. It seems that the shape of the curve beyond the critical angle is primarily determined by the absorption per layer thickness and by the velocity contrast.

2.3 The effect of introducing a thin layer in the upper sediment of the two-layer model

As has already been seen, a very thin layer (with respect to the wave length) has a negligible effect — it is nearly transparent. This was illustrated in Fig. 3.1 for a thin layer overlaying the lower, semi-infinite medium.

Such layers are often found in nature, especially when turbidity currents are responsible for the deposition. As an example of this it is interesting to analyze the case in which a thin layer is found within the upper medium of the two-layer bottom. The bottom now, in fact, is better characterized by a four-layer model.

Consider, therefore, the addition of an extra layer — $\lambda/16$ thick, for instance — and allow the location of this layer to change within the upper medium. For each position of this thin layer a certain reflection loss curve is obtained for the whole system. The envelopes of all these curves give the maximum deviation one can expect from the pure two-layer model without the extra layer.

The result of such a computation is shown in Fig. 17 — computed for two velocity contrasts — from which it is seen that, with velocity contrasts that are not too high, thin layers have little importance, no matter where they are located in the system.

This result is quite important, since from this one can often simplify the complicated models frequently obtained from cores or high frequency echo-soundings. In models that include a series of very thin layers it is possible to neglect these layers completely and thereby simplify the analysis.

2.4 The effect of the shear waves in the lower layer

The effect of shear waves on the reflection loss for a simple semi-infinite reflector is shown in Fig. 18. Two cases have been computed, one without absorption and the other one with the absorption of 1 db/λ.

As already mentioned, the computer programme permits computation of the reflection loss for a multi-layered reflector with shear waves in the lowest layer. The effect of shear waves in the lower medium of a two-layer bottom is shown in Fig. 19 for some different thicknesses of the upper layer and for some different shear wave velocities. In these cases absorption has not been included.

The shear wave velocity is certainly a very difficult parameter to measure in practice. Velocities from 0.05 - 0.3 times the compressional wave velocity seem to be typical for marine sediments (Refs. 6, 7). It is seen from Fig. 19 that such low shear velocities have a very small effect on the reflection loss.

If, on the other hand, the shear wave velocity in the lower medium is high (as in rock) the picture becomes quite complicated, as shown in Fig. 20.

The assumption that the shear velocity should be zero — or very close to zero — in the upper layer is probably true. The upper layers are nearly always considered completely fluid.

3. MEASURED REFLECTION COEFFICIENTS

The reflection loss for the ocean bottom has been measured over great areas of the Mediterranean Sea, using explosive sound sources and measuring the energy of the received signal reflected from the bottom. The angle of incidence was varied by varying the distance between the transmitting and receiving ships.

The energy was measured in octave bands between 75 and 4,800 cps. If the bottom can be characterized by a two-layer model, it should be possible, in one or two neighbouring filters, to observe a relatively high reflection loss if the layer thickness is about a quarter wave length. The effect should be very pronounced if the layer thickness is a quarter wave length at the centre frequency of one of the octave bands. For the above filters this means layer thicknesses in the range 10 cm - 4 m.

These effects have actually been observed in the measurements. Figure 21 shows results of a measurement where the reflection losses at vertical incidence are not very different in the different filters (Ref. 8). On the contrary, the results given in Fig. 22 show very clearly a higher reflection loss in the lowest filter (75 - 150 cps), which might mean a layering of the sediments with an upper layer thickness of some few metres. Actually, this case seems to be at least as common as the case shown in Fig. 21 where the reflection loss does not vary with frequency. It should be emphasized that the results shown in Fig. 21 and 22 are average results from quite large areas.

Some coring has been carried out, but not deep enough to verify the acoustic measurements. However, in an area with acoustic results very similar to the results shown in Fig. 22 — indicating an upper layer some few metres thick — most of the core contained fine mud, while at the bottom (at about 3.5 m) a sand layer showed up. Because of the shortness of the core it is uncertain whether this sand layer is only thin or whether it stretches to greater depths. A core from the area that gave the results in Fig. 21 (frequency independent reflection loss) showed a much more sandy sediment extending right to the top. Deeper cores will probably be taken in the very near future.

In Fig. 23 an attempt has been made to fit some measured points to a theoretical computation of the reflection loss for a two-layer reflector. The parameters used in this computation are not measured ones, but a trial and error method has been used in which a certain relationship between density and sound velocity has been taken into account.

The well-known relationship between sound velocity and porosity (which determines the density) (Ref. 9) is shown in Fig. 24, which also shows some measured points obtained from the cores.

CONCLUSION

The purpose of this work has been to make a systematic, theoretical survey of the reflection loss from a two-layer reflector.

It has been seen that the shape of the curve showing the reflection loss vs. angle of incidence is very characteristic for a given layer thickness and should be easily recognizable.

Absorption alters the curves, especially around and beyond the critical angle, its effect being mostly to diminish the oscillations in the curves. Absorption in the lower layer has much less effect than that in the upper layer.

Wide angle measurements with a harmonic source should be very useful. If a broad band source is used, a Fourier analysis is to be preferred to energy measurements in broad frequency bands, since otherwise many interesting effects are averaged out. However, layers which are about a quarter wave length thick can be — and probably have been — detected using explosive sound sources analyzed in octave bands.

Shear waves in the lower layer of the two-layer model have a negligible effect on the reflection loss for the low shear wave velocities expected to exist in porous marine sediments.

Layers that are thin with respect to the wave length are practically transparent.

A useful supplement to this theoretical work would be to investigate the effect of velocity gradients in the layers.

Programmes to compute both the pulse distortion upon reflection from a layered reflector and the reflection coefficient with shear waves in all the layers are being prepared by O. Hastrup and will make a natural conclusion to the present theoretical work on layered bottoms.

REFERENCES

1. B.F. Cole, "Marine Sediment Attenuation and Ocean Bottom Reflected Sound", paper presented at the 68th meeting of the Acoustical Society of America. Austin, Texas, October 1964.

2. F.R. Menotti, W.R. Schumacher, S.R. Santaniello, "Studies of Observed and Predicted Values of Bottom Reflectivity as a Function of Incident Angle", paper presented at the 68th meeting of the Acoustical Society of America. Austin, Texas, October 1964.

3. G.R. Bernard, J.L. Bardin, W.B. Hempkins, "Underwater Sound Reflection from Layered Media", J.A.S.A., Vol. 36, No. 11, p. 2119, November 1964.

4. Brekhovskikh, "Waves in Layered Media", Academic Press, 1960.

5. P.H. Smith, "An Improved Transmission Line Calculator", Electronics, 17 January 1944, p. 130.

6. J.E. Nafe and C.L. Drake, "Variation with Depth in Shallow and Deep Water Marine Sediments of Porosity, Density and the Velocities of Compressional and Shear Waves", Geophysics, Vol. XXII, July 1957, p. 523.

7. H.P. Bucker, J.A. Whitney, D.L. Keir, "Use of Stoneley Waves to Determine the Shear Velocity in Ocean Sediments", J.A.S.A., Vol. 36, No. 8, August 1964, p. 1595.

8. B. Lallement and P. Stangerup, "Reflectivity of Deep Sedimentary Bottoms", paper presented at the 68th meeting of the Acoustical Society of America. Austin, Texas, October 1964.

9. E.L. Hamilton, "Low Sound Velocities in High Porosity Sediments", J.A.S.A. Vol. 28, No. 1, January 1956, p. 16.

Analogy between Sound Reflection from the Ocean Bottom and Reflection from a Discontinuity in a Transmission Line

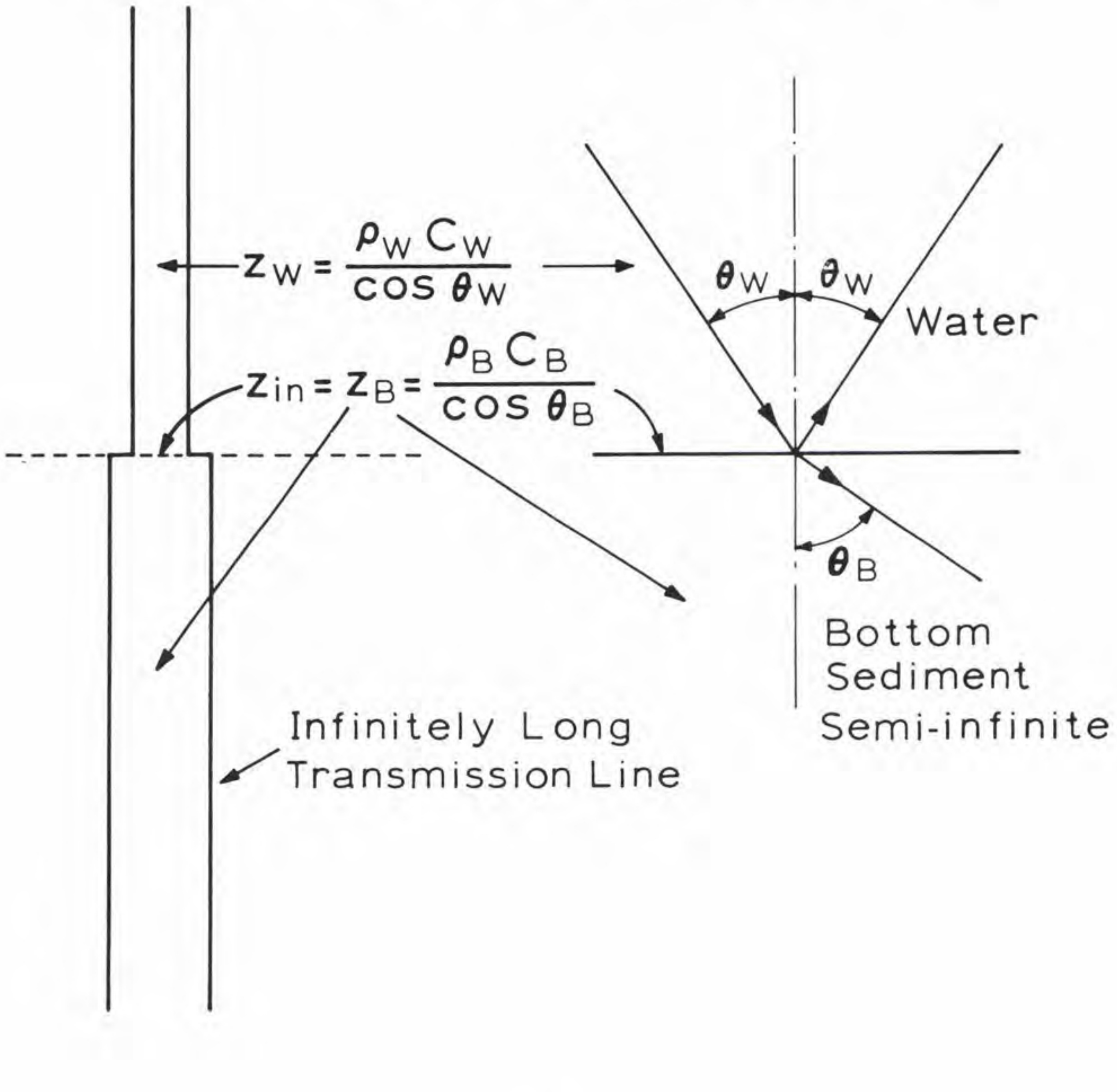

Fig. 1

n-Layered Bottom Model

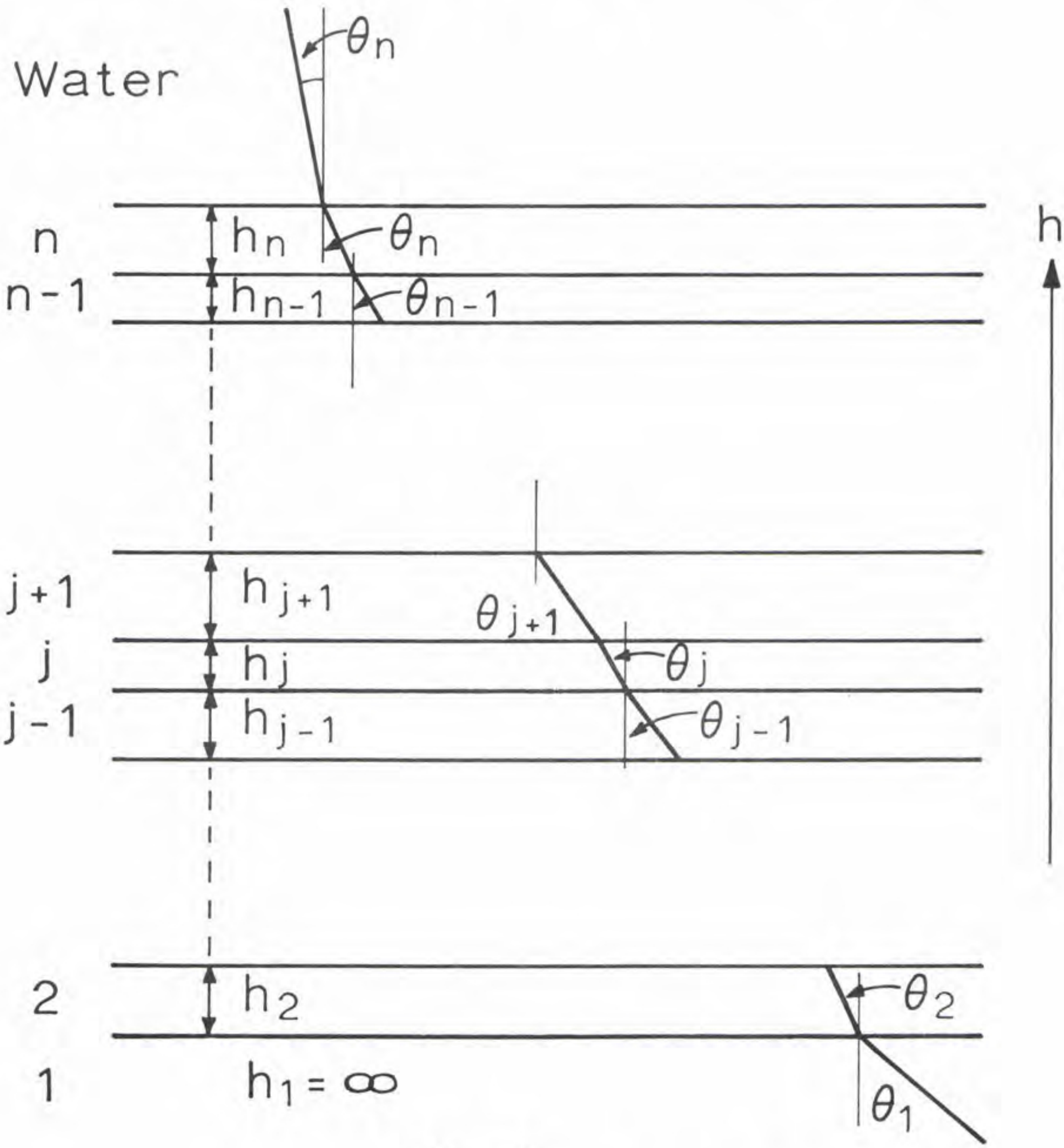

$$Z_{in}^{(j)} = \frac{Z_{in}^{(j-1)} - iZ_j \tan \emptyset_j}{Z_j - iZ_{in}^{(j-1)} \tan \emptyset_j} Z_j$$

$$\emptyset_j = k_j h_j \cos \theta_j$$

Fig. 2

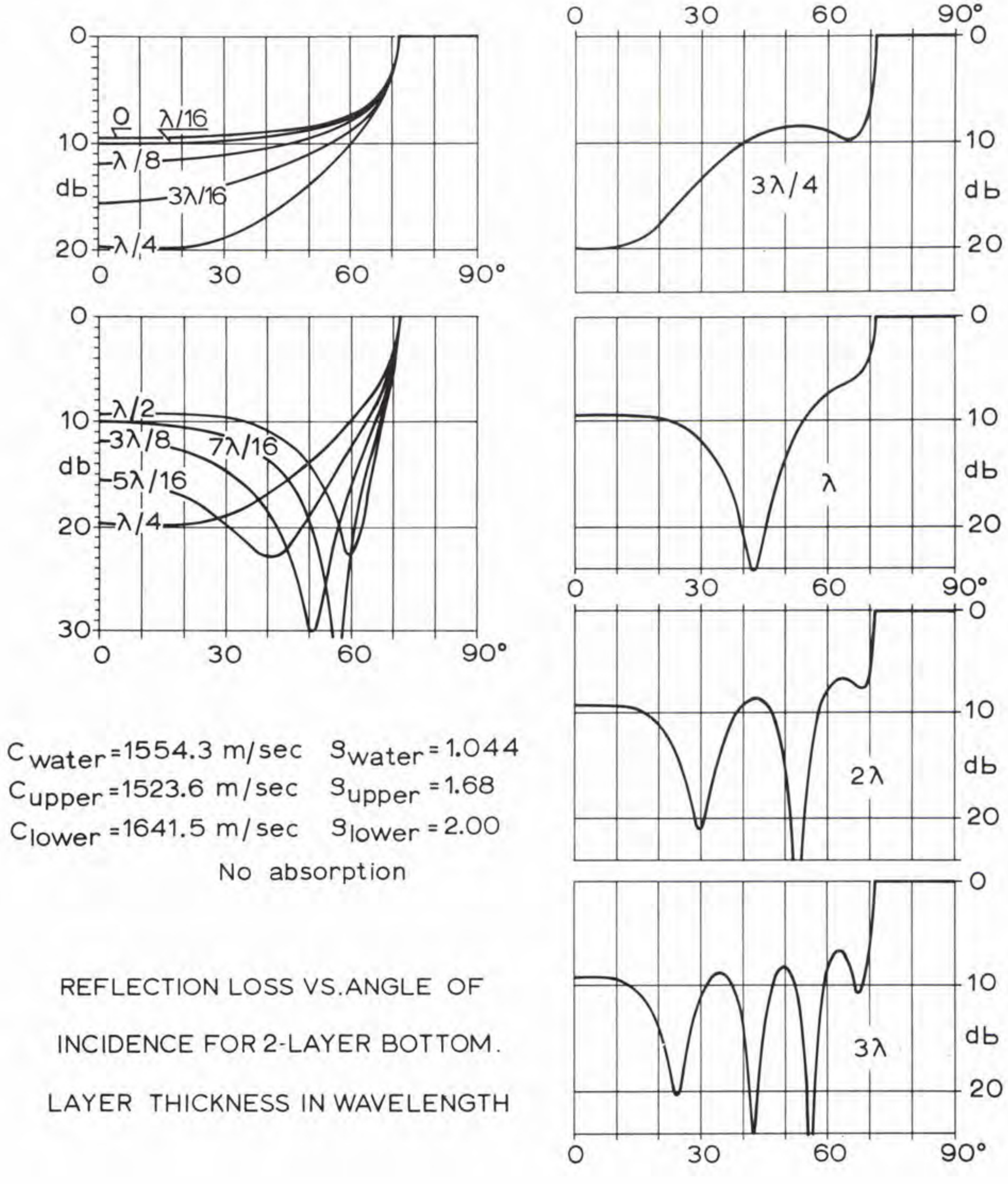

REFLECTION LOSS VS. ANGLE OF INCIDENCE FOR 2-LAYER BOTTOM. LAYER THICKNESS IN WAVELENGTH

Fig. 3

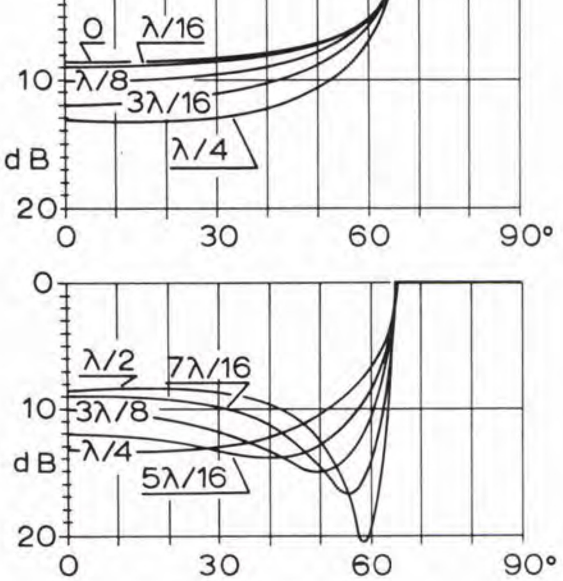

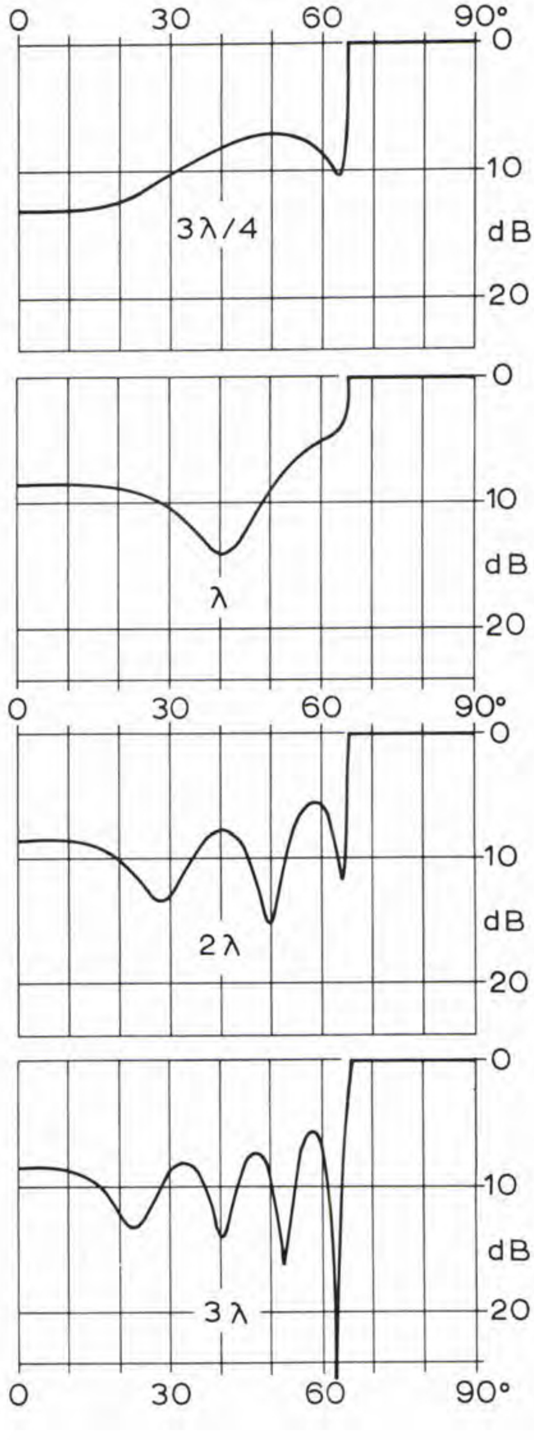

C_{water} = 1554.3 m/sec ρ_{water} = 1.044
C_{upper} = 1591.1 m/sec ρ_{upper} = 1.9
C_{lower} = 1708.3 m/sec ρ_{lower} = 2.1
No absorption

REFLECTION LOSS VS ANGLE OF

INCIDENCE FOR 2-LAYER BOTTOM.

LAYER THICKNESS IN WAVELENGTH

Fig. 4

REFLECTION LOSS V.S. ANGLE OF INCIDENCE FOR 2-LAYER BOTTOM

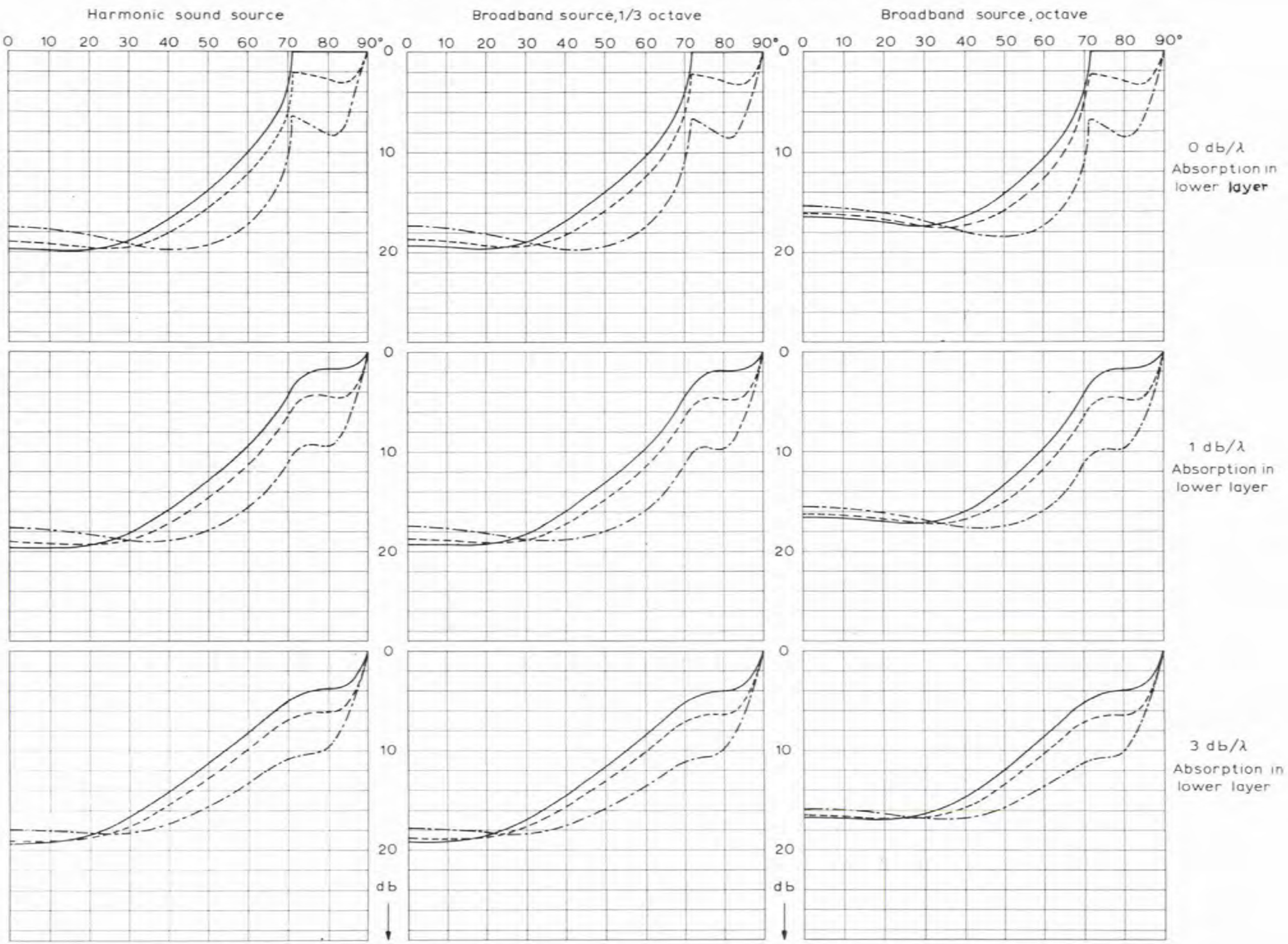

C_{water} = 1554.3 m/sec ρ_{water} = 1.044
C_{upper} = 1523.6 m/sec ρ_{upper} = 1.68
C_{lower} = 1641.5 m/sec ρ_{lower} = 2.00

λ/4 LAYER

Fig. 5

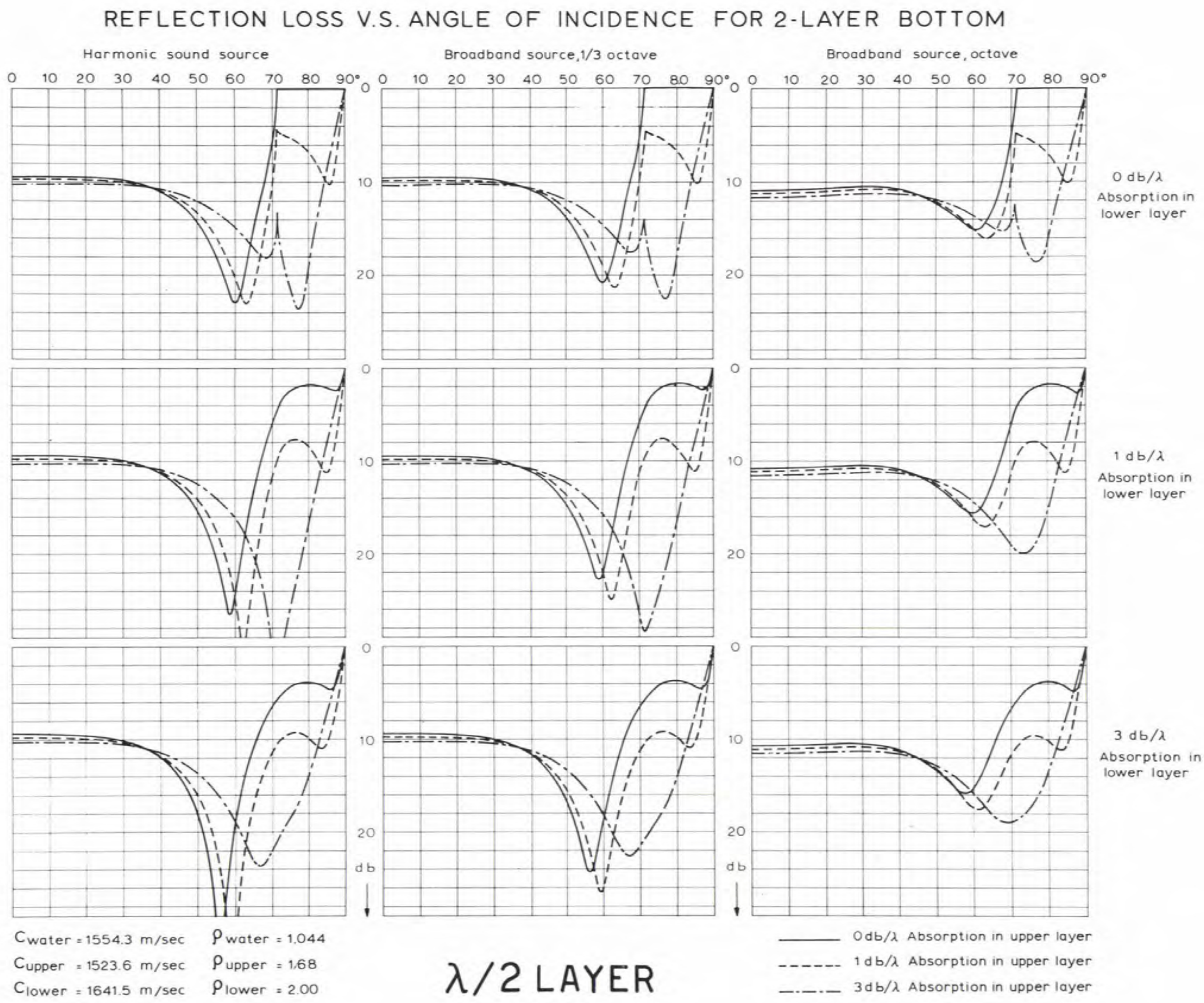

REFLECTION LOSS V.S. ANGLE OF INCIDENCE FOR 2-LAYER BOTTOM
Harmonic sound source
Broadband source, 1/3 octave
Broadband source, octave
0 10 20 30 40 50 60 70 80 90°
0 10 20
db
0 db/λ Absorption in lower layer
1 db/λ Absorption in lower layer
3 db/λ Absorption in lower layer
C_{water} = 1554.3 m/sec
C_{upper} = 1523.6 m/sec
C_{lower} = 1641.5 m/sec
ρ_{water} = 1.044
ρ_{upper} = 1.68
ρ_{lower} = 2.00
0 db/λ Absorption in upper layer
1 db/λ Absorption in upper layer
3 db/λ Absorption in upper layer
λ/2 LAYER

Fig. 6

REFLECTION LOSS V.S. ANGLE OF INCIDENCE FOR 2-LAYER BOTTOM

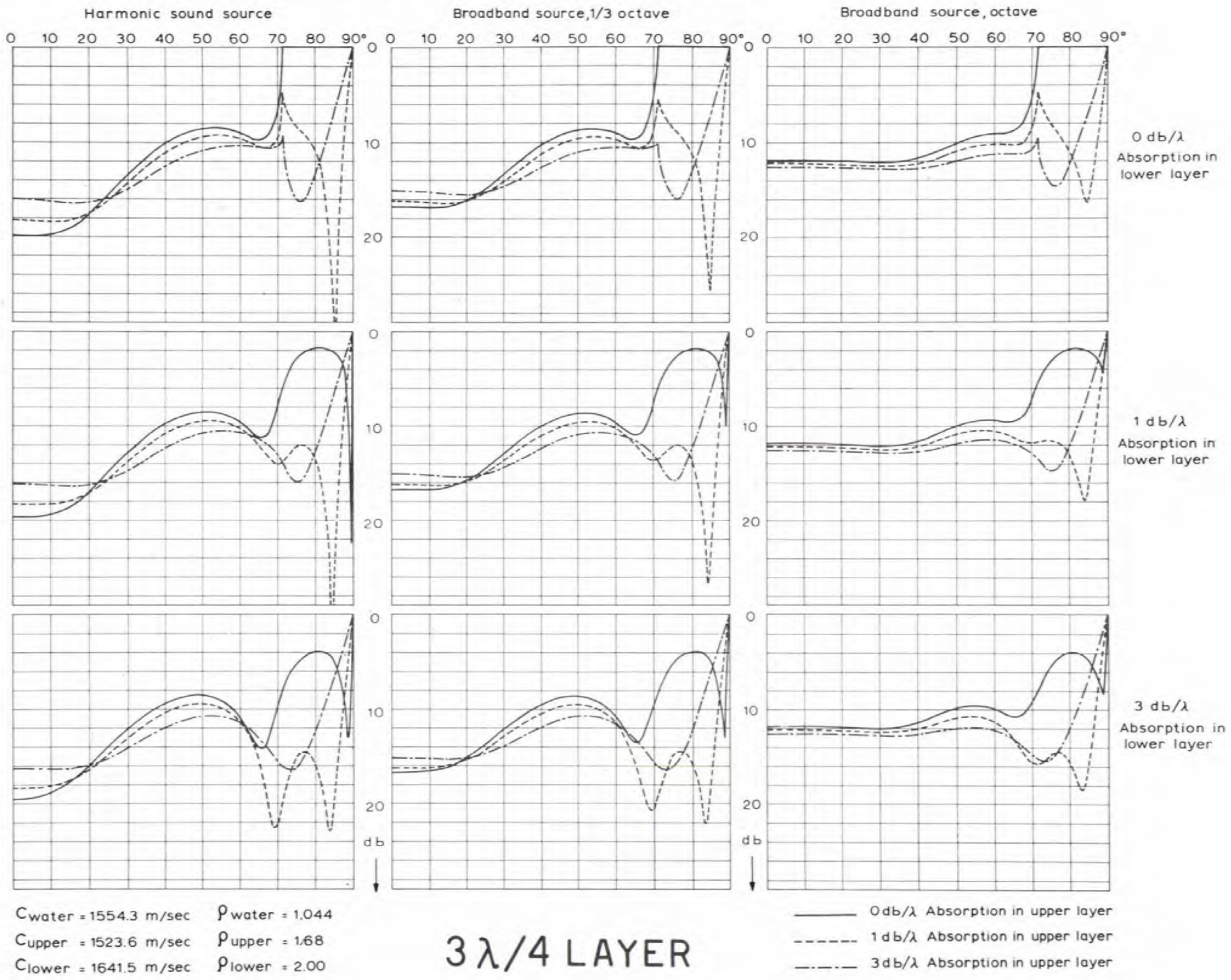

3λ/4 LAYER

Fig. 7

REFLECTION LOSS V.S. ANGLE OF INCIDENCE FOR 2-LAYER BOTTOM

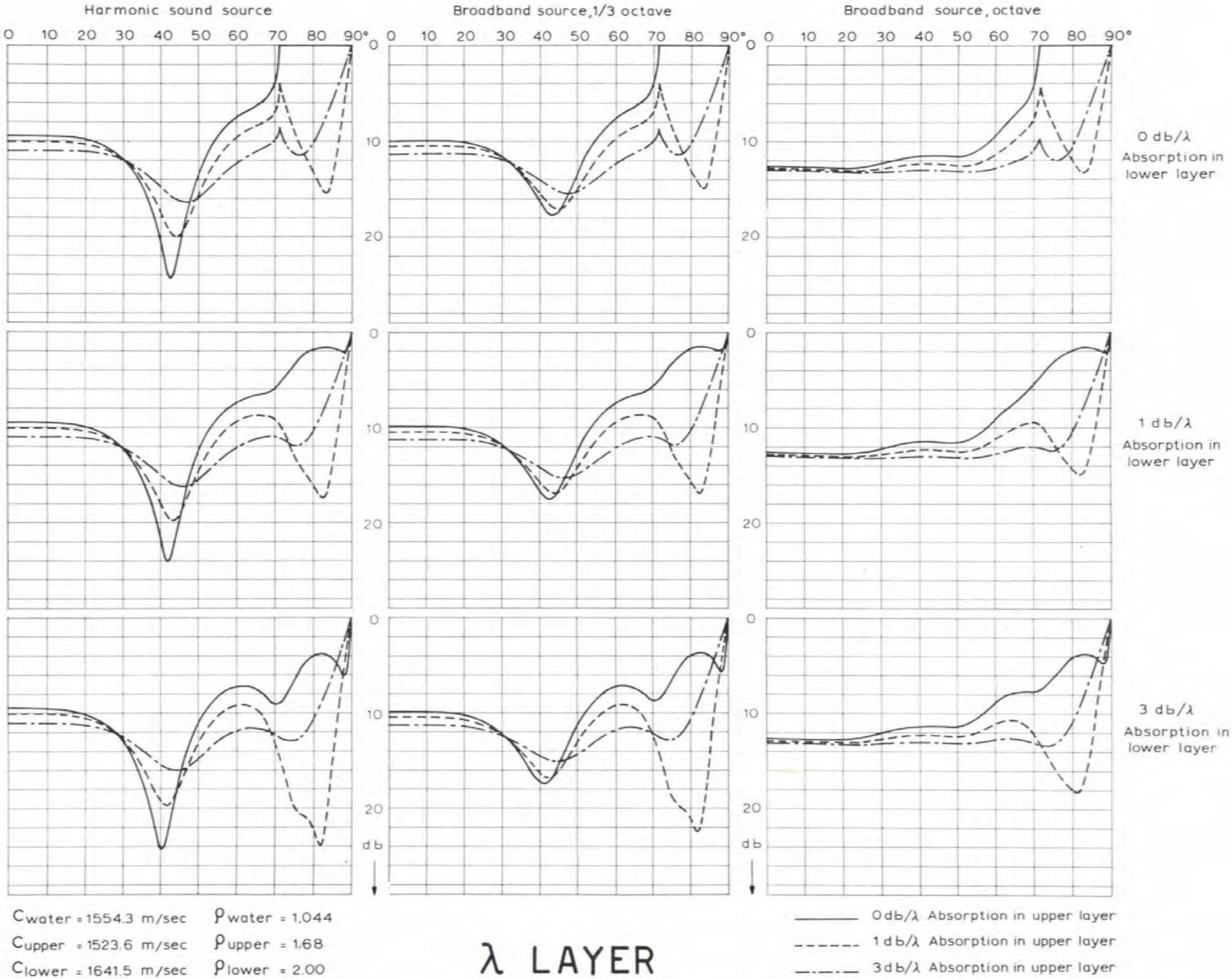

λ LAYER

Fig. 8

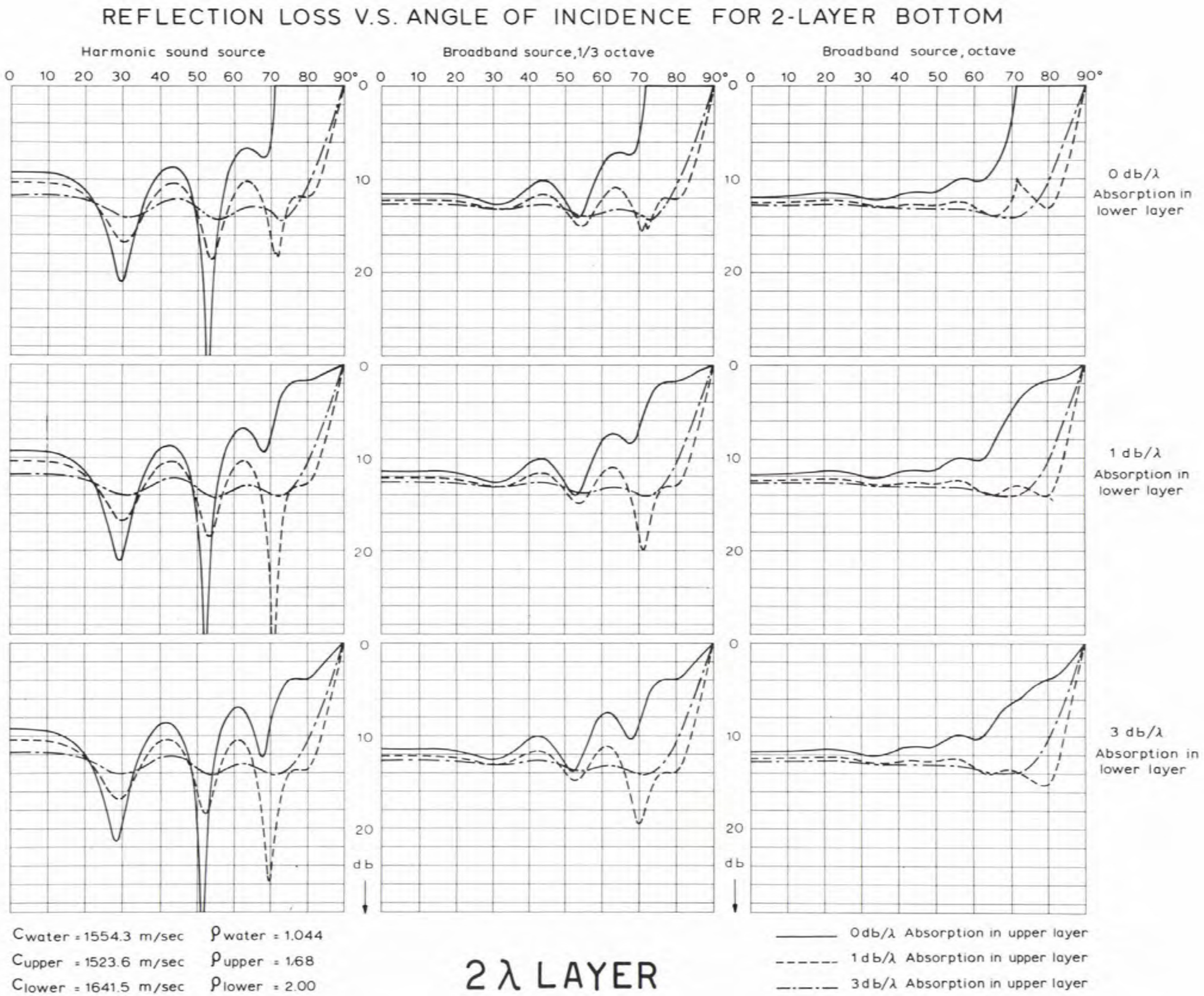
REFLECTION LOSS V.S. ANGLE OF INCIDENCE FOR 2-LAYER BOTTOM
Harmonic sound source
Broadband source, 1/3 octave
Broadband source, octave
0 10 20 30 40 50 60 70 80 90°
0 10 20
db
0 db/λ Absorption in lower layer
1 db/λ Absorption in lower layer
3 db/λ Absorption in lower layer
C_{water} = 1554.3 m/sec ρ_{water} = 1.044
C_{upper} = 1523.6 m/sec ρ_{upper} = 1.68
C_{lower} = 1641.5 m/sec ρ_{lower} = 2.00
0 db/λ Absorption in upper layer
1 db/λ Absorption in upper layer
3 db/λ Absorption in upper layer
2λ LAYER

Fig. 9

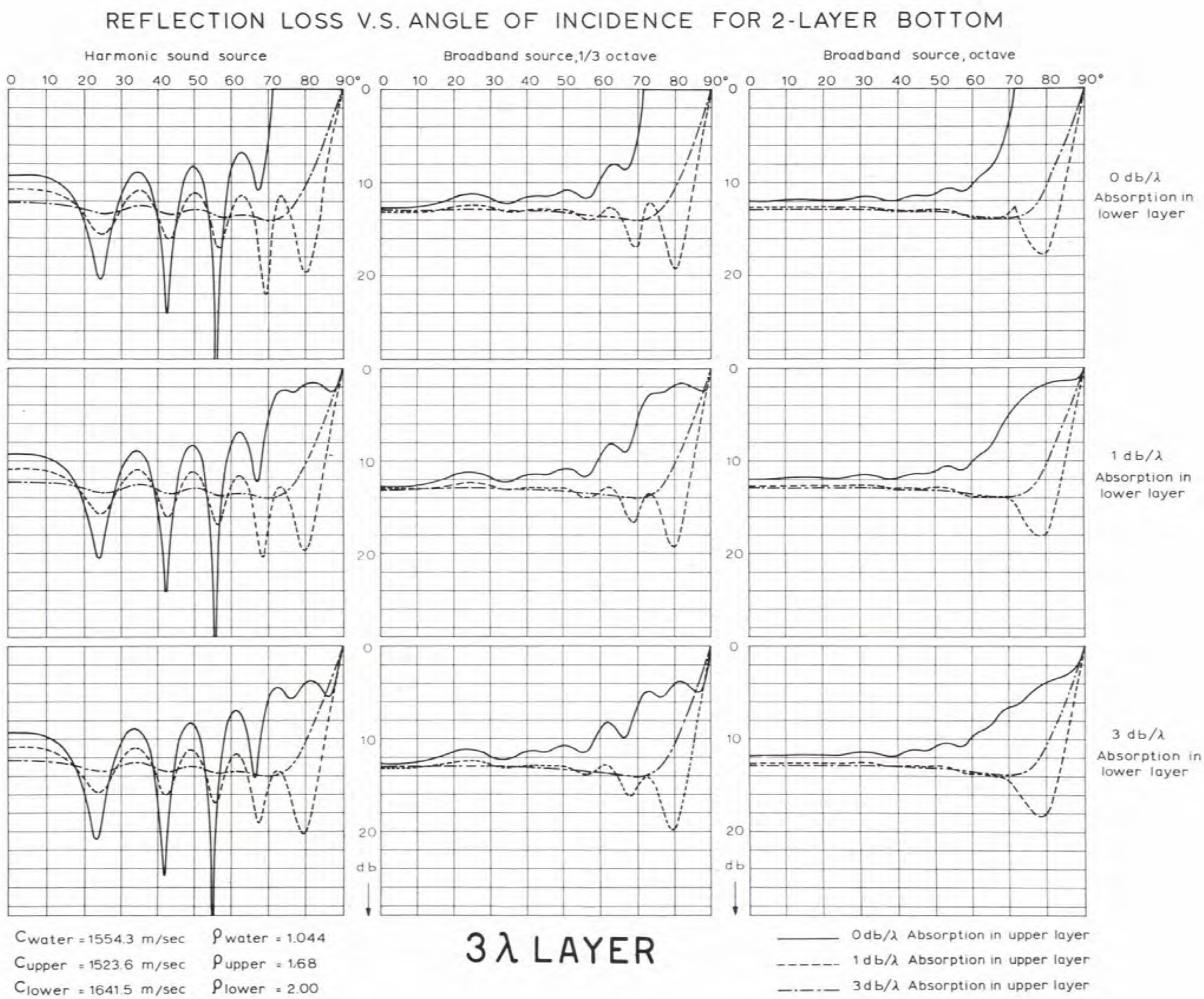

REFLECTION LOSS V.S. ANGLE OF INCIDENCE FOR 2-LAYER BOTTOM
Harmonic sound source
Broadband source,1/3 octave
Broadband source, octave
0 10 20 30 40 50 60 70 80 90°
0 10 20
db
0 db/λ Absorption in lower layer
1 db/λ Absorption in lower layer
3 db/λ Absorption in lower layer
Cwater = 1554.3 m/sec
Cupper = 1523.6 m/sec
Clower = 1641.5 m/sec
ρwater = 1.044
ρupper = 1.68
ρlower = 2.00
3λ LAYER
0 db/λ Absorption in upper layer
1 db/λ Absorption in upper layer
3 db/λ Absorption in upper layer

Fig. 10

REFLECTION LOSS V:S. ANGLE OF INCIDENCE FOR 2-LAYER BOTTOM

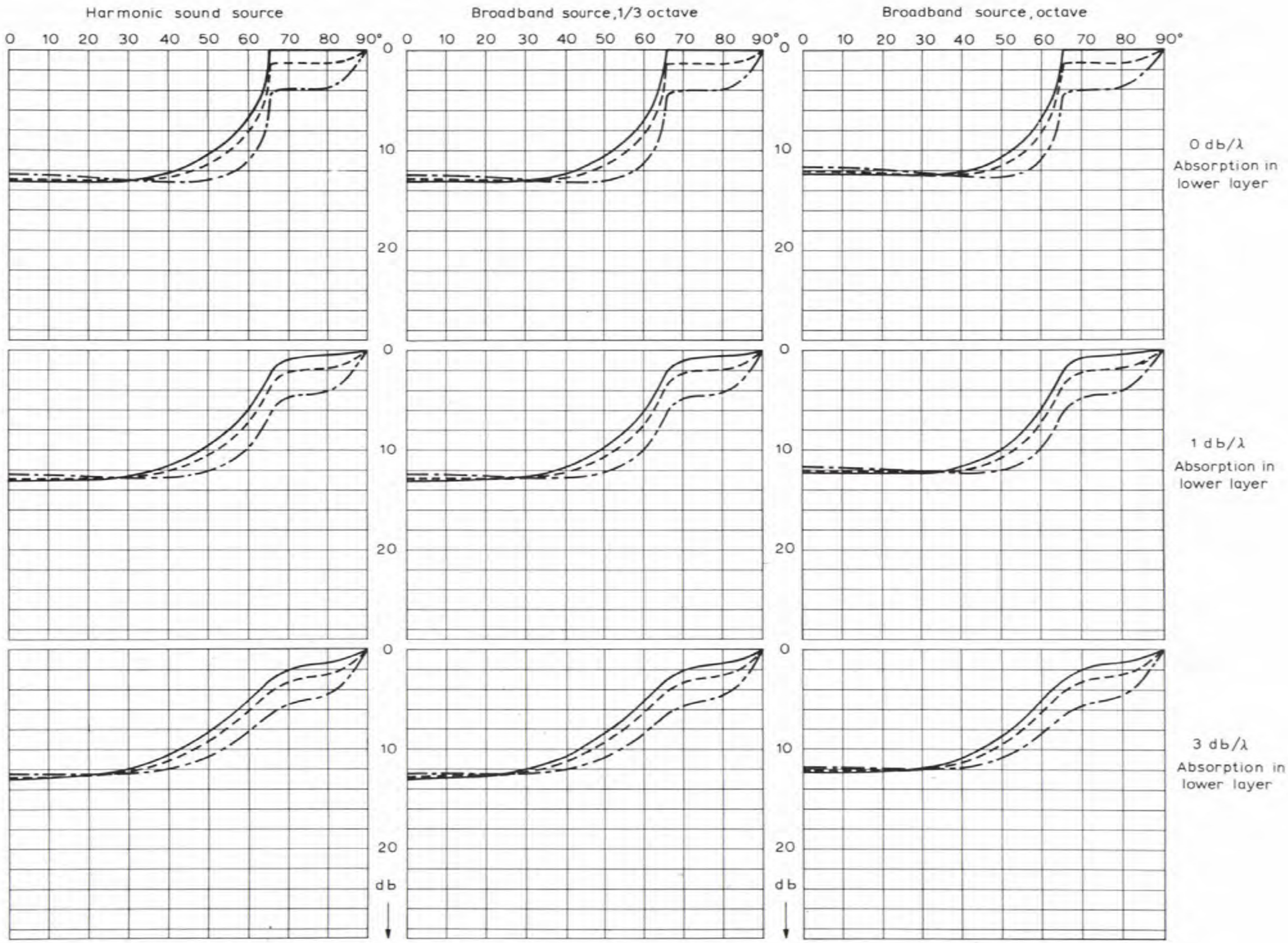

C_{water} = 1554.3 m/sec ρ_{water} = 1.044
C_{upper} = 1591.1 m/sec ρ_{upper} = 1.90
C_{lower} = 1708.3 m/sec ρ_{lower} = 2.10

λ/4 LAYER

Fig. 11

REFLECTION LOSS V.S. ANGLE OF INCIDENCE FOR 2-LAYER BOTTOM

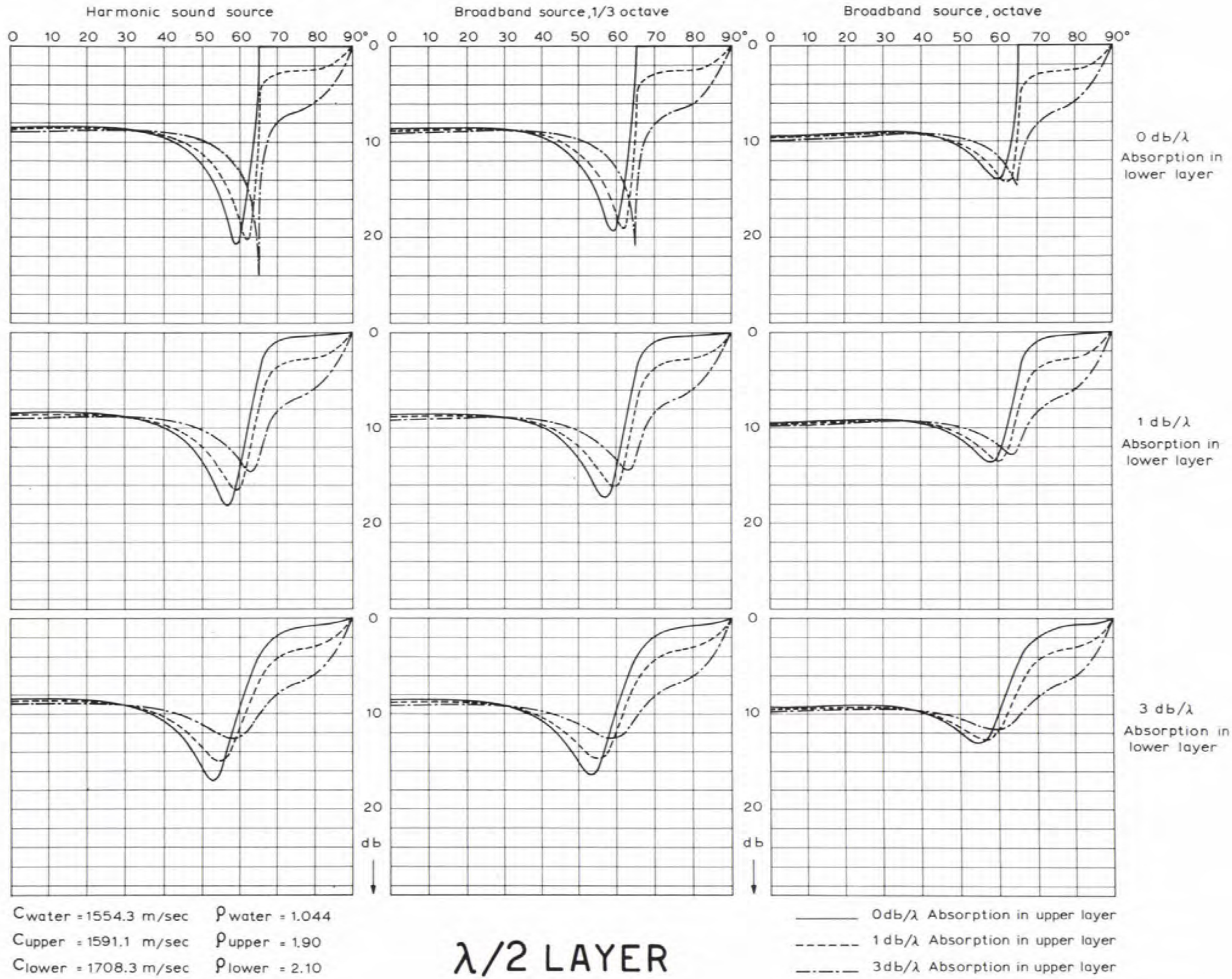

λ/2 LAYER

Fig. 12

REFLECTION LOSS V:S. ANGLE OF INCIDENCE FOR 2-LAYER BOTTOM

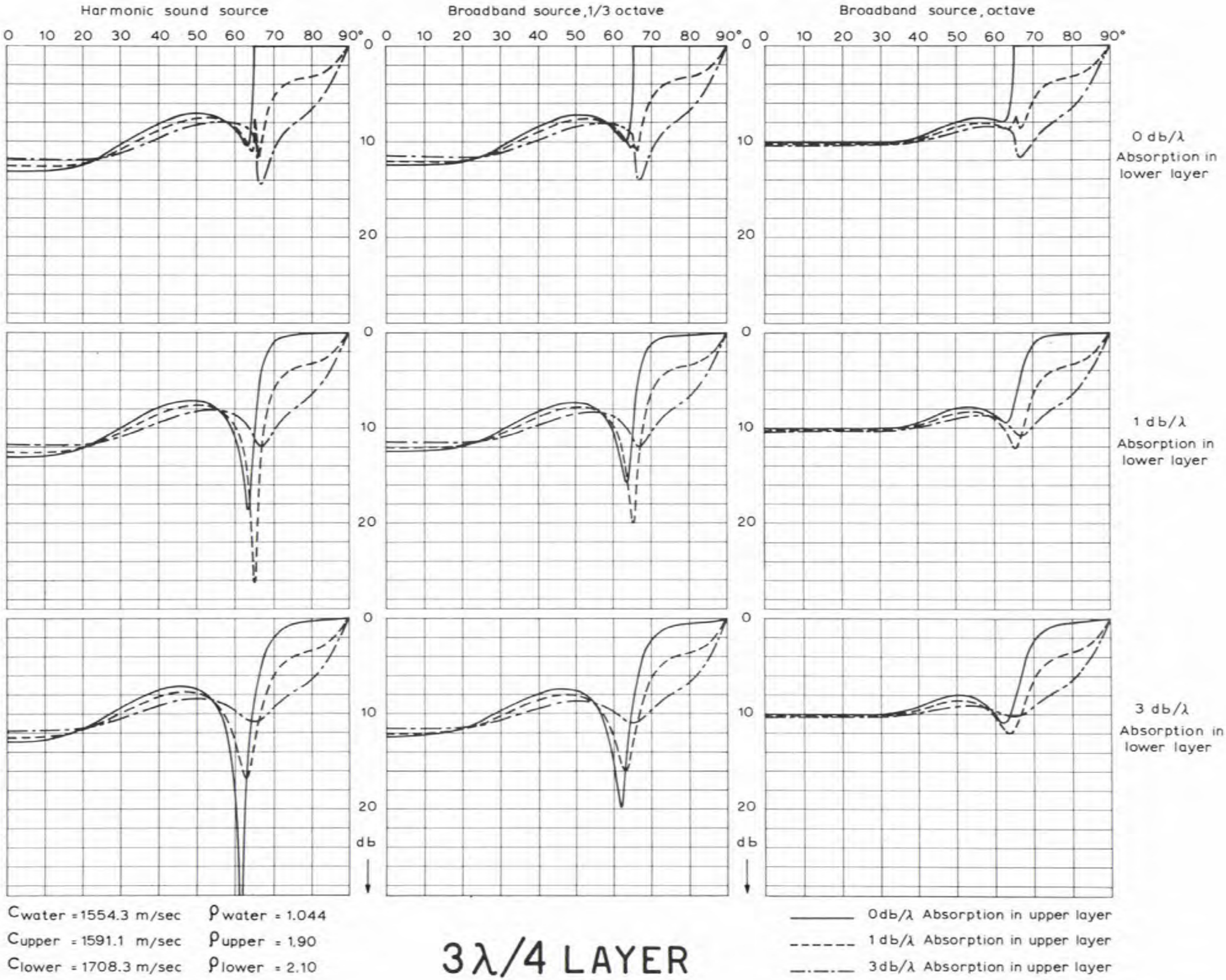

3λ/4 LAYER

Fig. 13

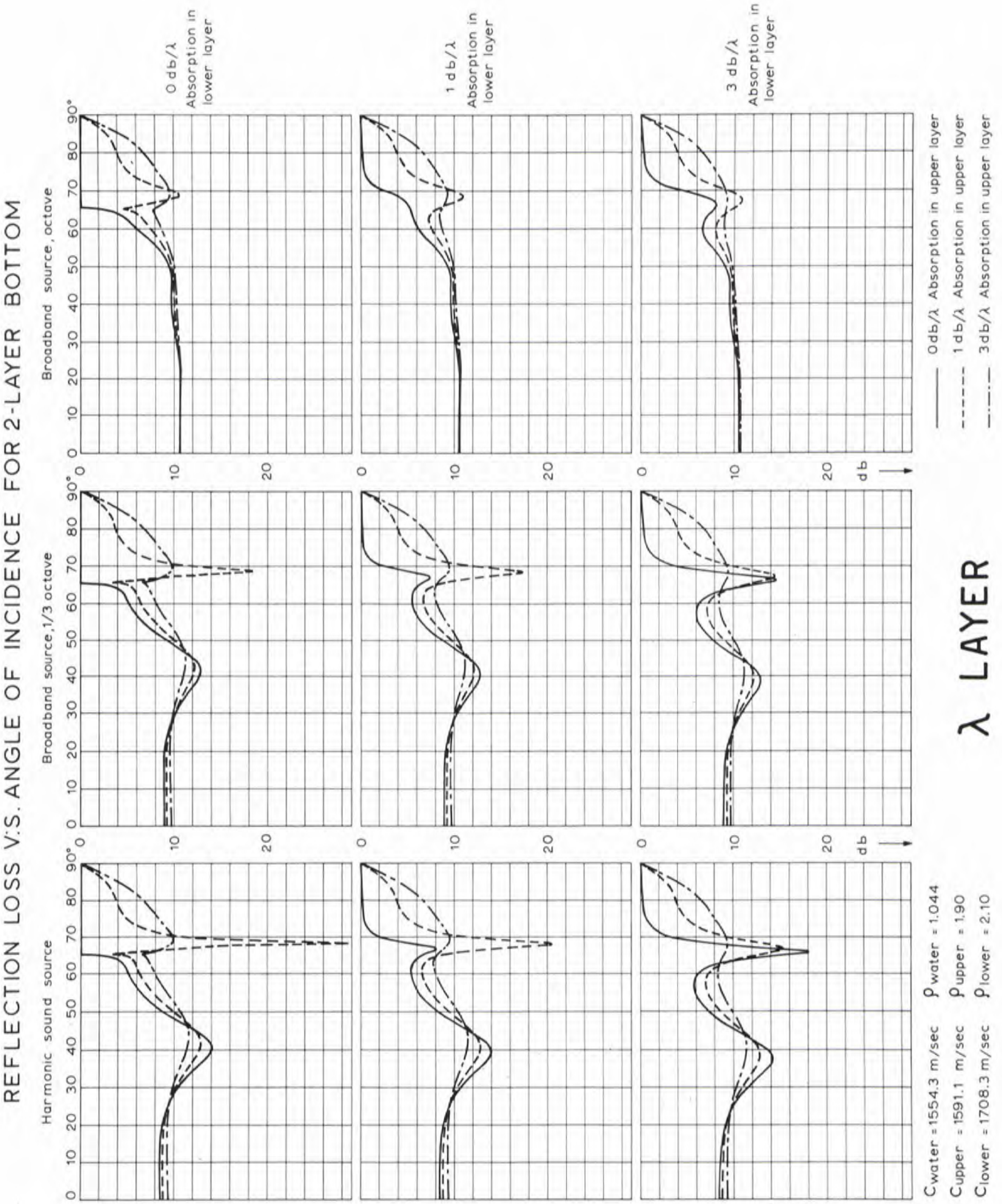
REFLECTION LOSS V:S. ANGLE OF INCIDENCE FOR 2-LAYER BOTTOM
Harmonic sound source
Broadband source, 1/3 octave
Broadband source, octave
0 db/λ Absorption in lower layer
1 db/λ Absorption in lower layer
3 db/λ Absorption in lower layer
db
0db/λ Absorption in upper layer
1 db/λ Absorption in upper layer
3 db/λ Absorption in upper layer
Cwater = 1554.3 m/sec
Cupper = 1591.1 m/sec
Clower = 1708.3 m/sec
ρwater = 1.044
ρupper = 1.90
ρlower = 2.10
λ LAYER

Fig. 14

REFLECTION LOSS V:S. ANGLE OF INCIDENCE FOR 2-LAYER BOTTOM

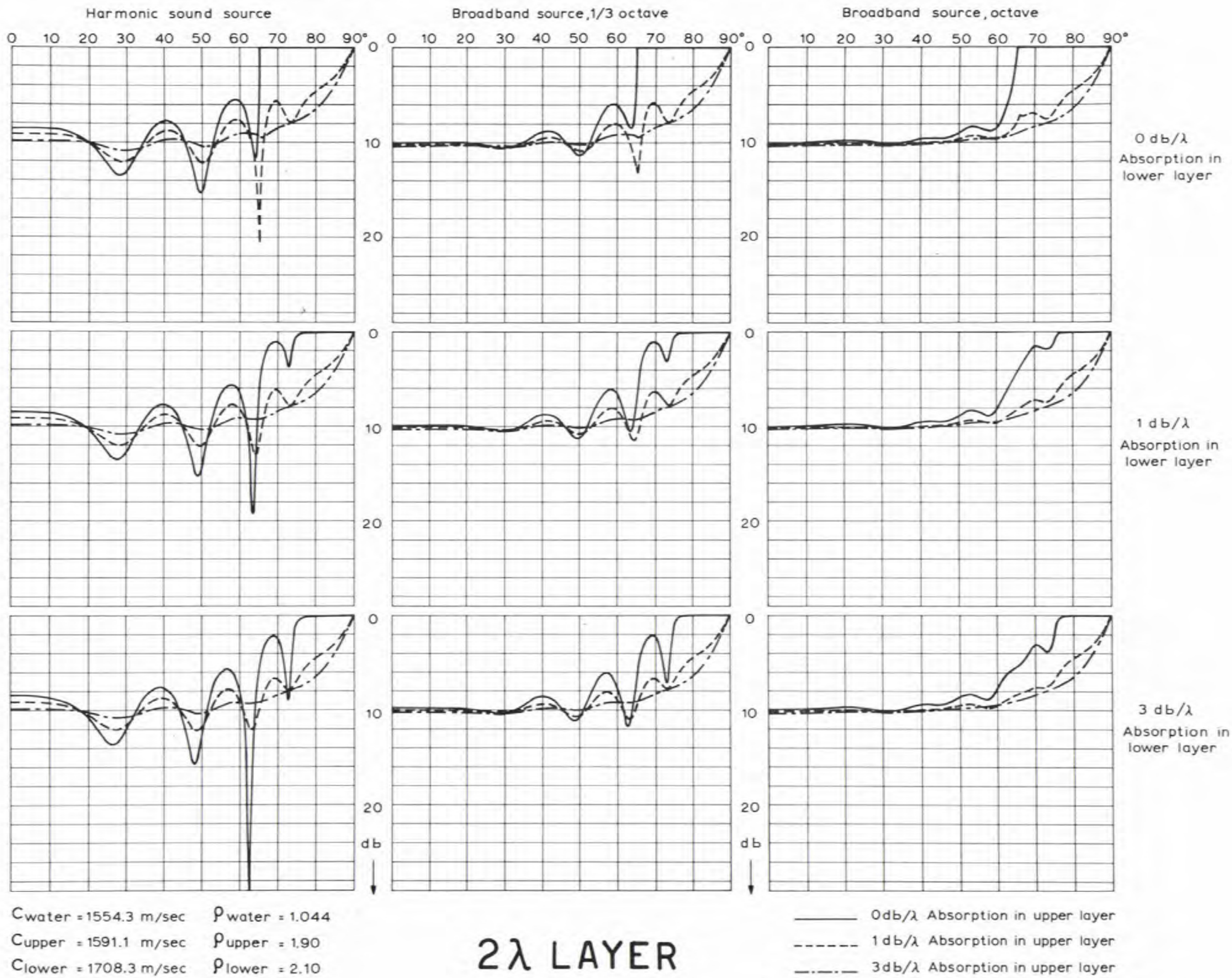

2λ LAYER

Fig. 15

REFLECTION LOSS V.S. ANGLE OF INCIDENCE FOR 2-LAYER BOTTOM

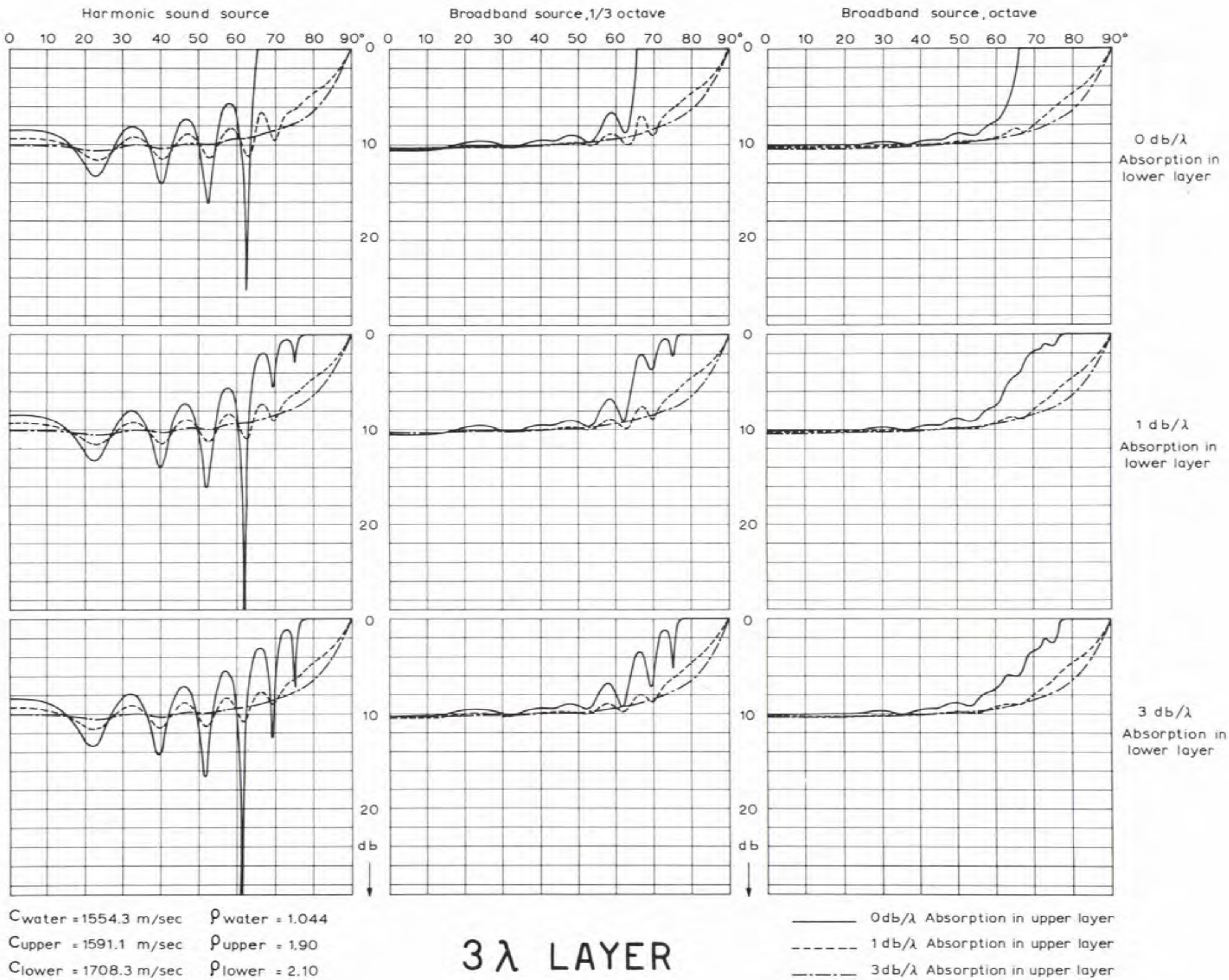

3λ LAYER

Fig. 16

EFFECT OF INTRODUCING A THIN LAYER IN THE UPPER SEDIMENT OF THE 2-LAYER BOTTOM —

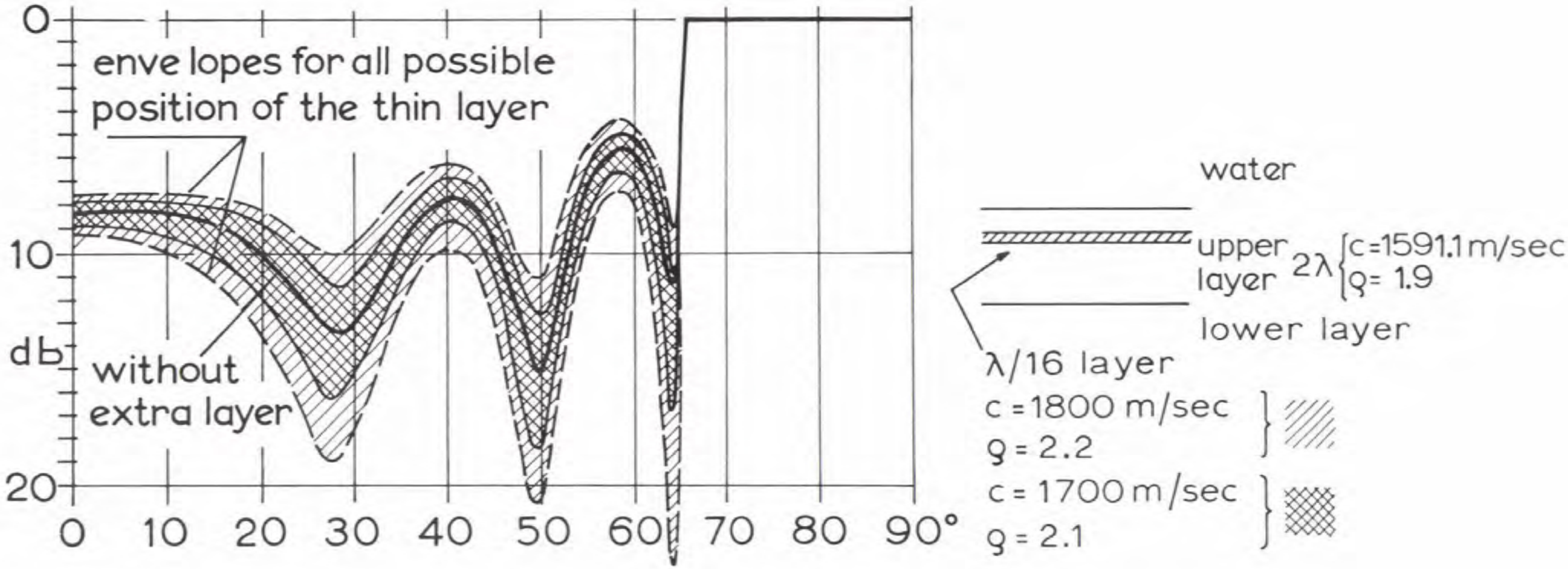

Fig. 17

REFLECTION LOSS VS. ANGLE OF INCIDENCE FROM A MEDIUM WITH SHEARWAVES

$C_S = k \times C_p$

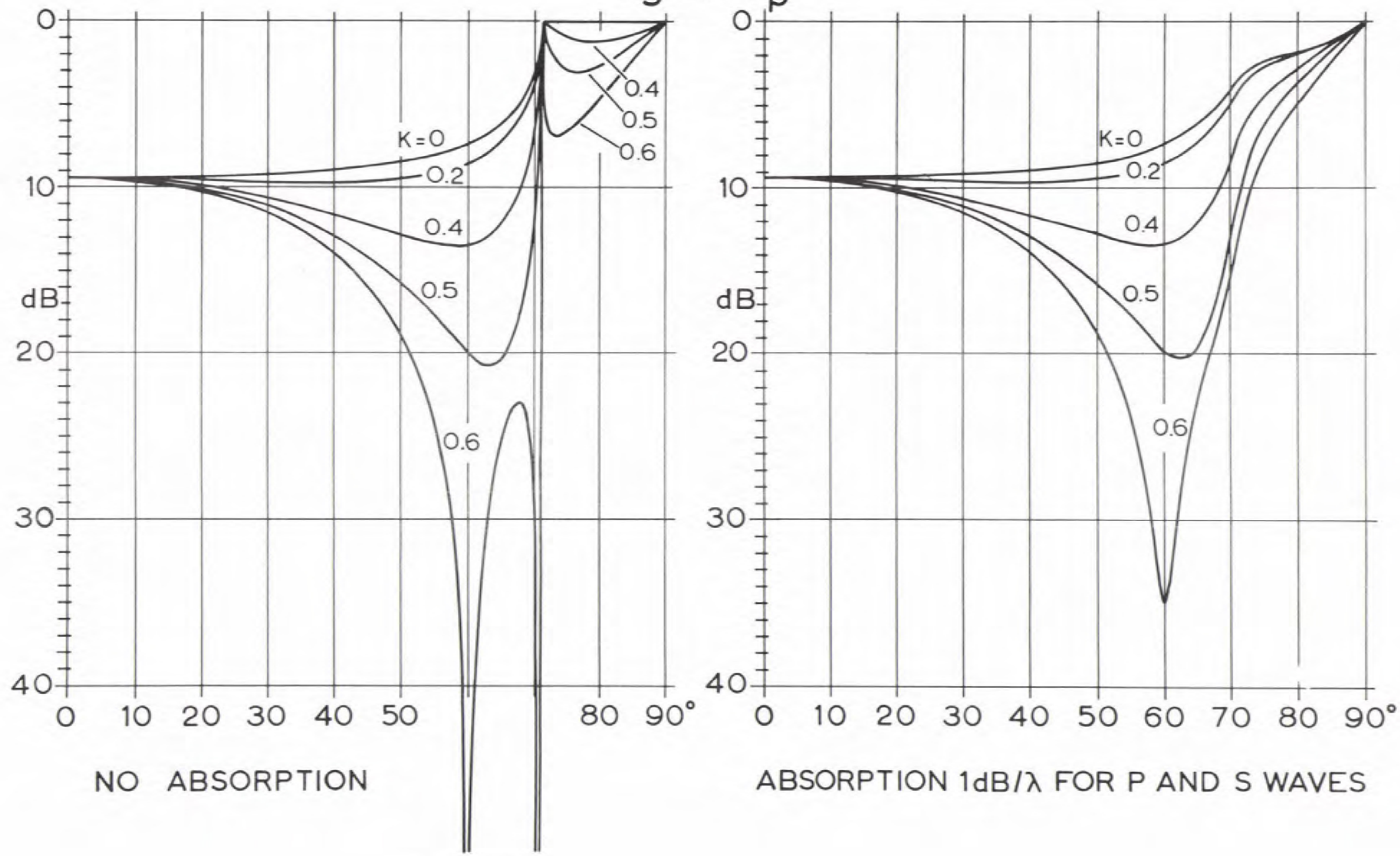

Fig. 18

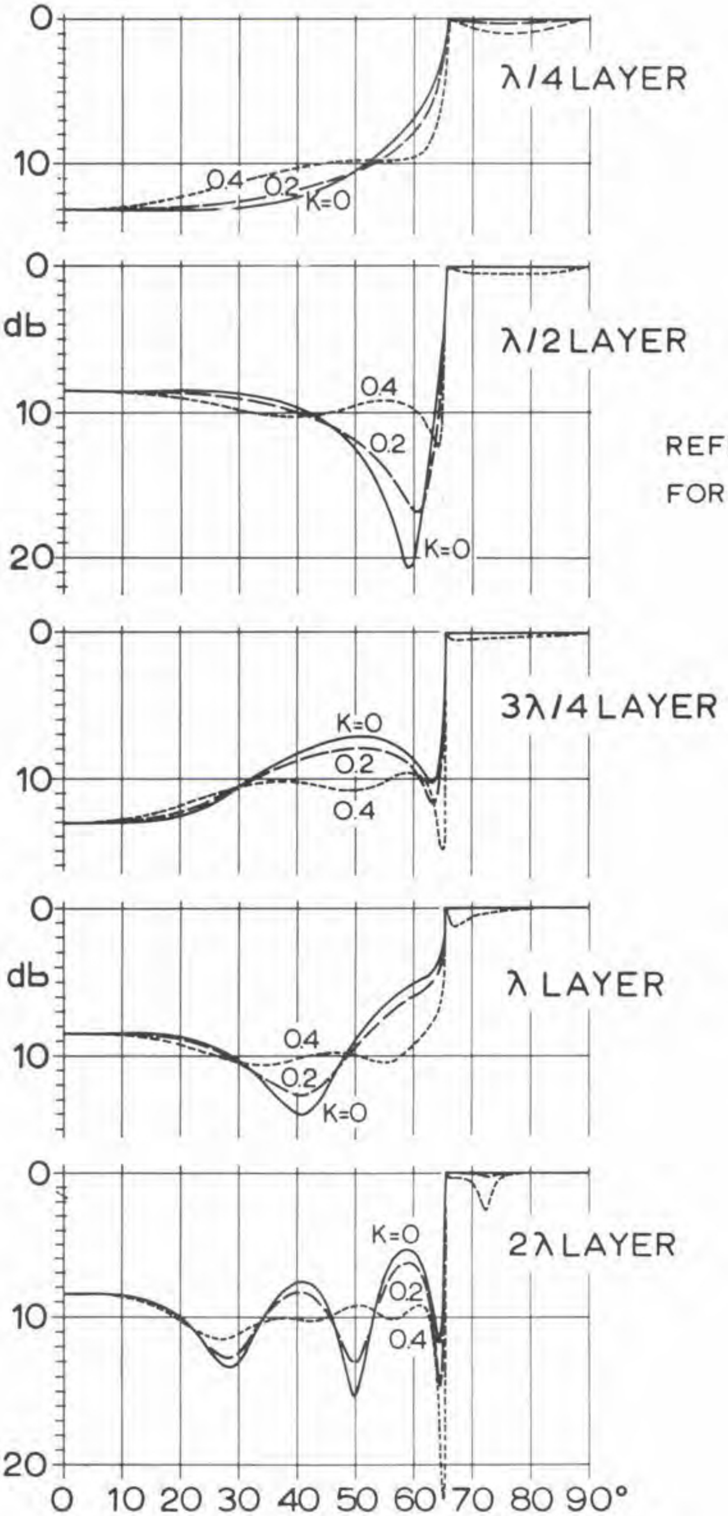

REFLECTION LOSS VS. ANGLE OF INCIDENCE FOR A TWO-LAYER BOTTOM WITH SHEAR IN THE LOWEST LAYER

$C_{water} = 1554.3 \text{ m/sec}$ $\rho_{water} = 1.044$

$C_{upper} = 1591.1 \text{ m/sec}$ $\rho_{upper} = 1.9$

$C_{lower} = 1708.3 \text{ m/sec}$ $\rho_{lower} = 2.1$

$C_{shear} = k \times C_p$

Fig. 19

REFLECTION LOSS VS. ANGLE OF INCIDENCE FOR A TWO-LAYER BOTTOM WITH SHEAR IN THE LOWEST LAYER

$\lambda / 2$ LAYER

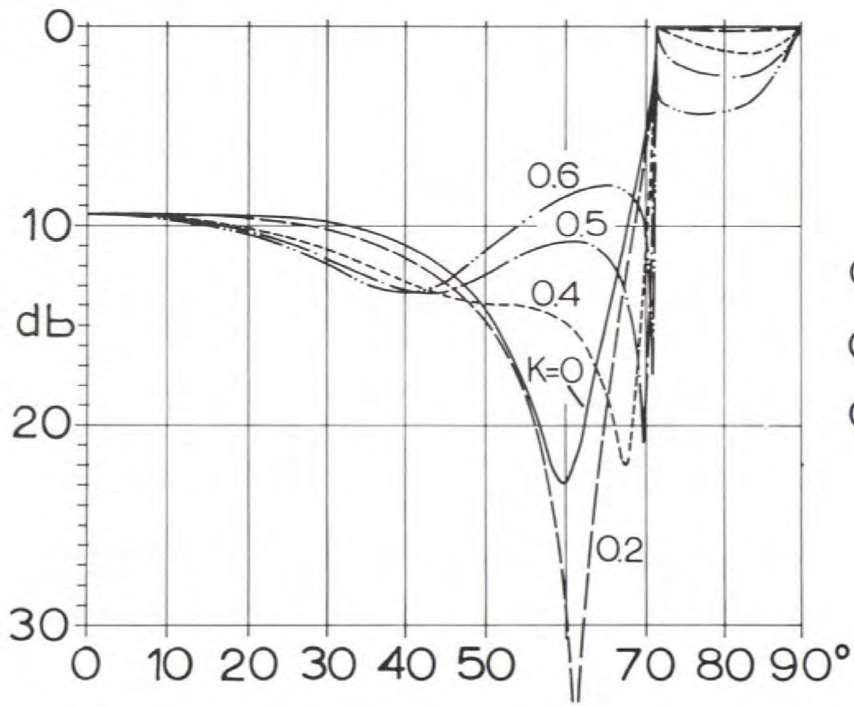

C_{water}=1554.3m/sec ρ_{water}=1.044

C_{upper}=1523.6m/sec ρ_{upper}=1.68

C_{lower}=1641.5m/sec ρ_{upper}=2.00

Fig. 20

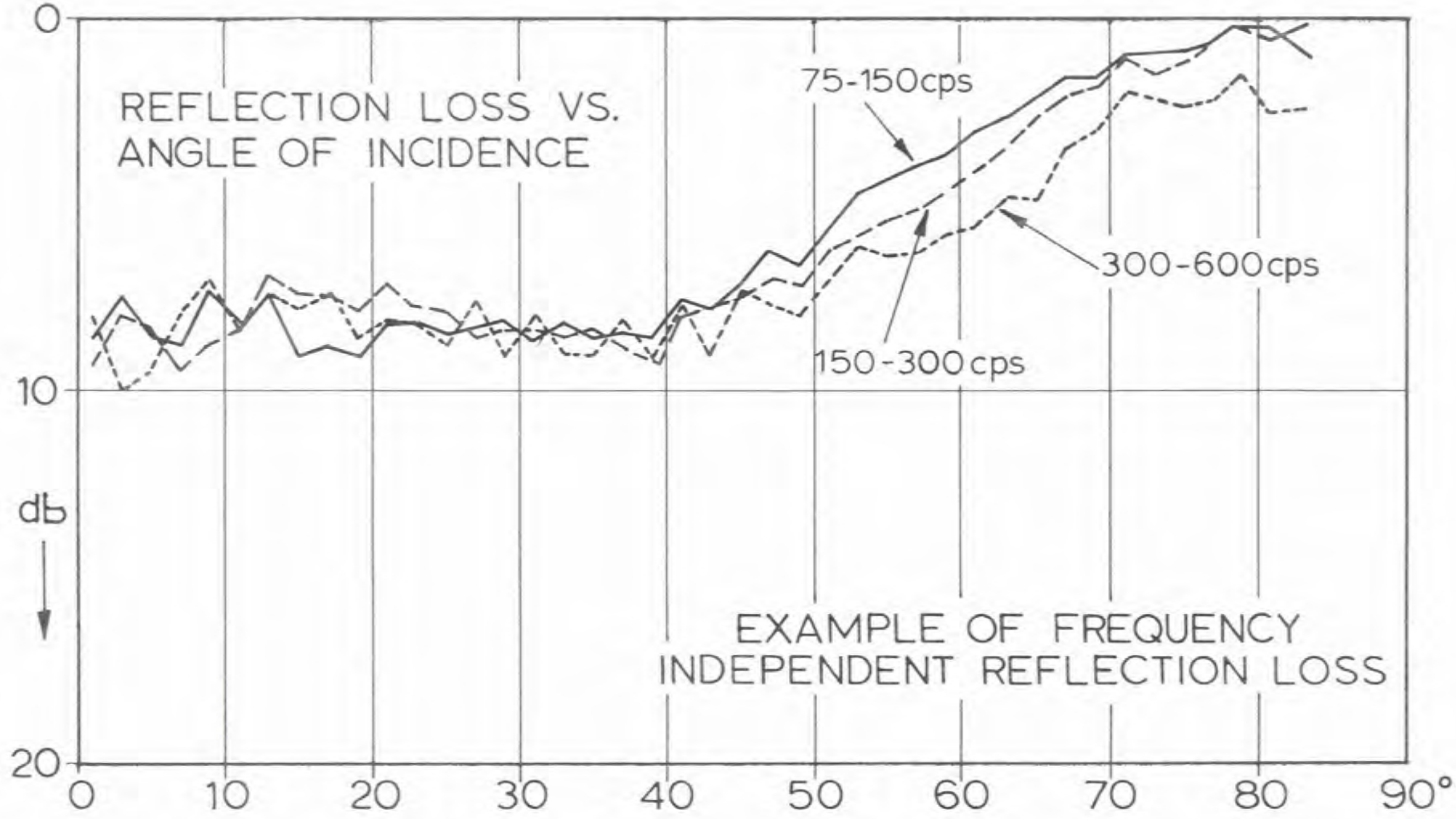

RESULTS OBTAINED FROM ENERGY MEASUREMENTS OF BROADBAND SOURCE IN OCTAVE BANDS

Fig. 21

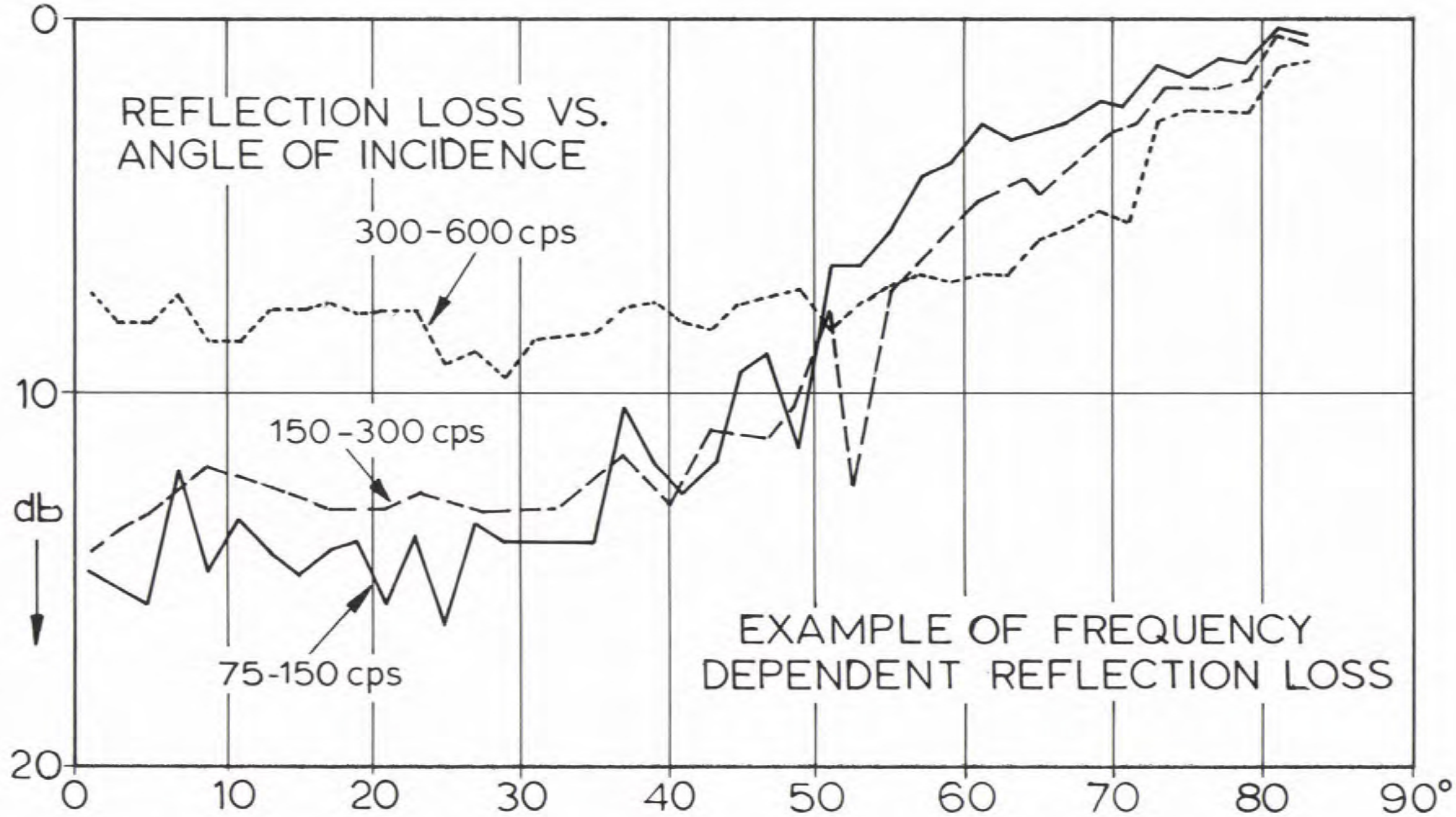

RESULTS OBTAINED FROM ENERGY MEASUREMENTS
OF BROADBANDS SOURCE IN OCTAVE BANDS

Fig. 22

COMPARISON BETWEEN MEASURED AND COMPUTED REFLECTION LOSS, ASSUMING A TWO-LAYER BOTTOM

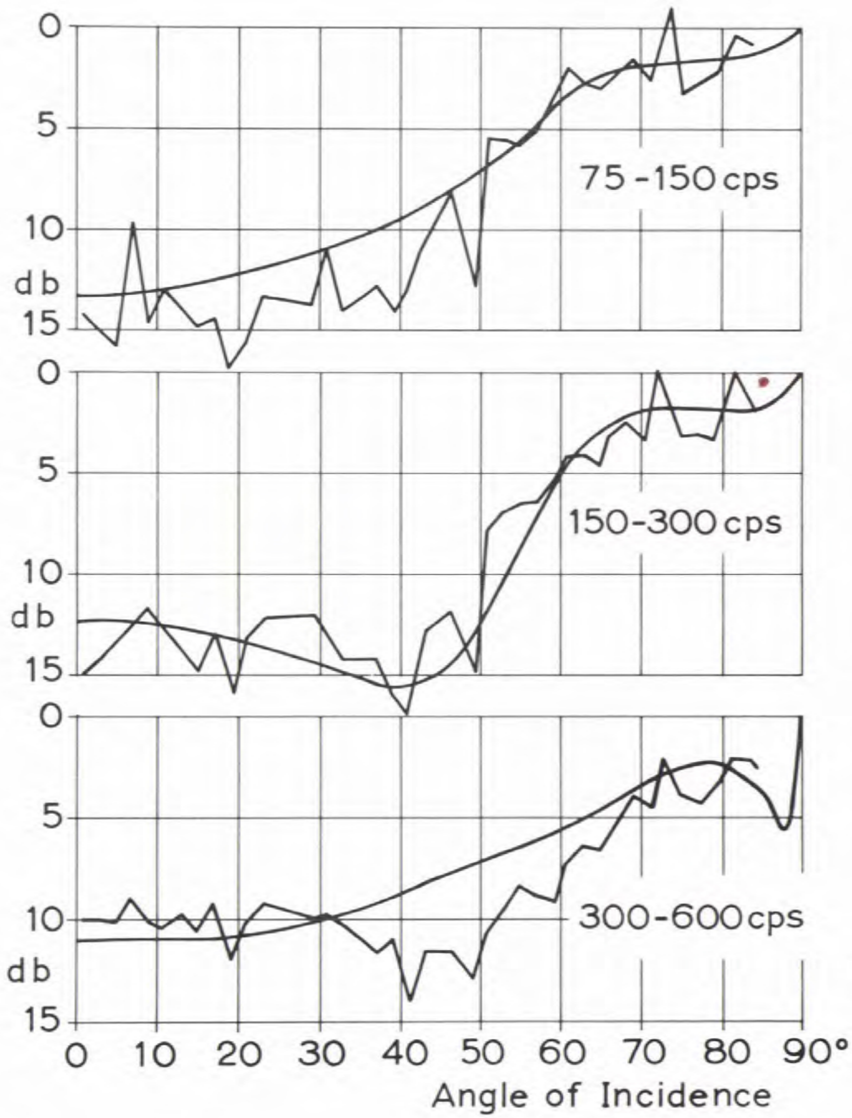

Velocity

C_{WATER} = 1554,3 m/sec

C_{UPPER} = 1518,1 m/sec

C_{LOWER} = 1780 m/sec

Density

ρ_{WATER} = 1,044

ρ_{UPPER} = 1,66

ρ_{LOWER} = 2,1

Absorption

a_{WATER} = 0 db/λ

a_{UPPER} = 0,15 db/λ

a_{LOWER} = 2,25 db/λ

Layer Thickness h = 2,35m

Fig. 23

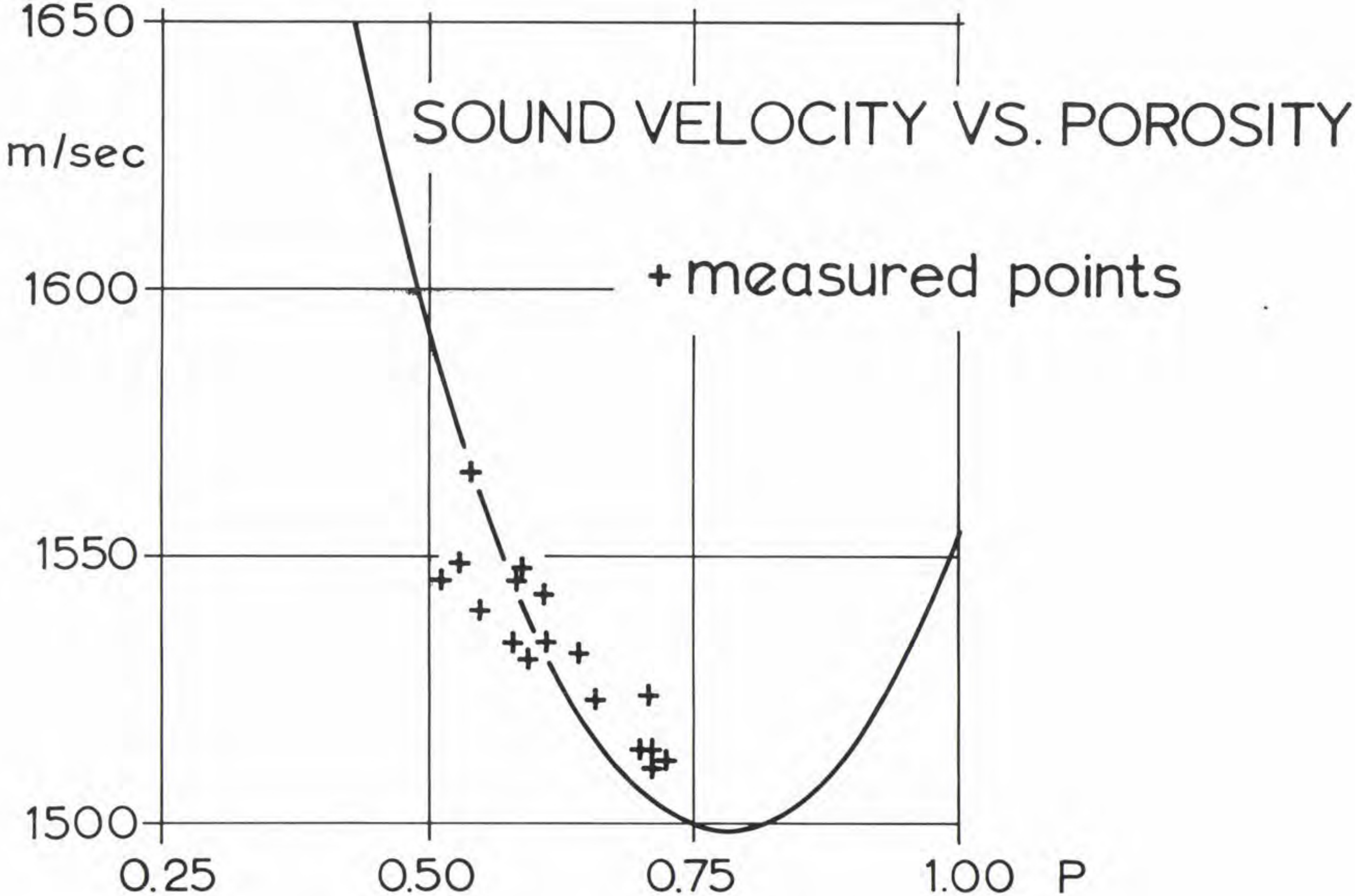
SOUND VELOCITY VS. POROSITY
+ measured points
m/sec
1650
1600
1550
1500
0.25
0.50
0.75
1.00
P

Fig. 24

D I S T R I B U T I O N   L I S T

Minister of Defense Brussels, Belgium	10 copies
Minister of National Defense Department of National Defense Ottawa, Canada	10 copies
Chief of Defense, Denmark Kastellet Copenhagen Ø, Denmark	10 copies
Minister of National Defense Division Transmissione-Ecoute-Radar 51 Latour Maubourg Paris 7e, France	10 copies
Minister of Defense Federal Republic of Germany Bonn, Germany	10 copies
Minister of Defense Athens, Greece	10 copies
Ministero della Difesa Stato Maggiore Marina Roma, Italy	10 copies
Minister of National Defense Plein 4, The Hague, Netherlands	10 copies
Minister of National Defense Storgaten 33, Oslo, Norway	10 copies
Minister of National Defense Lisboa, Portugal	10 copies
Minister of National Defense Ankara, Turkey	10 copies
Minister of Defense London, England	20 copies
Supreme Allied Commander Atlantic (SACLANT) Norfolk 23511, Virginia	3 copies
SACLANT Representative in Europe (SACLANTREPEUR) Place du Marechal de Lattre de Tassigny Paris 16e, France	1 copy

Commander in Chief Western Atlantic Area (CINCWESTLANT) Norfolk 23511, Virginia	1 copy
Commander in Chief Eastern Atlantic Area (CINCEASTLANT) Eastbury Park, Northwood Middlesex, England	1 copy
Maritime Air Commander Eastern Atlantic Area (COMAIREASTLANT) R.A.F. Northwood Middlesex, England	1 copy
Commander Submarine Force Eastern Atlantic (COMSUBEASTLANT) Fort Blockhouse Gosport, Hants, England	1 copy
Commander, Canadian Atlantic (COMCANLANT) H.M.C. Dockyard Halifax, Nova Scotia	1 copy
Commander Ocean Sub-Area (COMOCEANLANT) Norfolk 23511, Virginia	1 copy
Supreme Allied Commander Europe (SACEUR) Paris, France	7 copies
SHAPE Technical Center P.O. Box 174 Stadhouders Plantsoen 15 The Hague, Netherlands	1 copy
Allied Commander in Chief Channel (CINCCHAN) Fort Southwick, Fareham Hampshire, England	1 copy
Commander Allied Maritime Air Force Channel (COMAIRCHAN) Northwood, England	1 copy
Commander in Chief Allied Forces Mediterranean (CINCAFMED) Malta, G.C.	1 copy
Commander South East Mediterranean (COMEDSOUEAST) Malta, G.C.	1 copy

Commander Central Mediterranean (COMEDCENT) Naples, Italy	1 copy
Commander Submarine Allied Command Atlantic (COMSUBACLANT) Norfolk 23511, Virginia	1 copy
Commander Submarine Mediterranean (COMSUBMED) Malta, G.C.	1 copy
Standing Group, NATO (SGN) Room 2C256, The Pentagon Washington 25, D.C.	3 copies
Standing Group Representative (SGREP) Place du Marechal de Lattre de Tassigny Paris 16^{e}, France	5 copies
ASG for Scientific Affairs NATO Porte Dauphine Paris 16e, France	1 copy

National Liaison Representatives

NLR Belgium Belgian Military Mission 3330 Garfield Street, N.W. Washington, D.C.	1 copy
NLR Canada Canadian Joint Staff 2450 Massachusetts Avenue, N.W. Washington, D.C.	1 copy
NLR Denmark Danish Military Mission 3200 Massachusetts Avenue, N.W. Washington, D.C.	1 copy
NLR France French Military Mission 1759 "R" Street, N.W. Washington, D.C.	1 copy
NLR Germany German Military Mission 3215 Cathedral Avenue, N.W. Washington, D.C.	1 copy
NLR Greece Greek Military Mission 2228 Massachusetts Avenue, N.W. Washington, D.C.	1 copy
NLR Italy Italian Military Mission 3221 Garfield Street, N.W. Washington, D.C.	1 copy
NLR Netherlands Netherlands Joint Staff Mission 4200 Linneau Avenue Washington, D.C. 20008	1 copy
NLR Norway Norwegian Military Mission 2720 34th Street, N.W. Washington, D.C.	1 copy
NLR Portugal Portuguese Military Mission 2310 Tracy Place, N.W. Washington, D.C.	1 copy
NLR Turkey Turkish Joint Staff Mission 2125 LeRoy Place, N.W. Washington, D.C.	1 copy
NLR United Kingdom British Defence Staffs, Washington 3100 Massachusetts Avenue, N.W. Washington, D.C.	1 copy
NLR United States SACLANT Norfolk 23511, Virginia	40 copies

Scientific Committee of National Representatives

Dr. W. Petrie Defence Research Board Department of National Defence Ottawa, Canada	1 copy
G. Meunier Ingenieur en Chef des Genie Maritime Services Technique des Constructions et Armes Navales 8 Boulevard Victor Paris 15^{e}, France	1 copy
Dr. E. Schulze Bundesministerium der Verteidigung ABT H ROMAN 2/3 Bonn, Germany	1 copy
Commander A. Pettas Ministry of National Defense Athens, Greece	1 copy
Professor Dr. M. Federici Segreteria NATO MARIPERMAN La Spezia	1 copy
Dr. M.W. Van Batenburg Physisch Laboratorium RVO-TNO Waalsdorpvlakte The Hague, Netherlands	1 copy

Mr. A.W. Ross
Director of Naval Physical Research
Ministry of Defence (Naval)
Bank Block
Old Admiralty Building
Whitehall, London S.W. 1 — 1 copy

Dr. J.E. Henderson
Applied Physics Laboratory
University of Washington
1013 Northeast 40th Street
Seattle 5, Washington — 1 copy

Capitaine de Fregate R.C. Lambert
Etat Major Général Force Navale
Caserne Prince Baudouin
Place Dailly
Bruxelles, Belgique — 1 copy

CAPT H. L. Prause
Søvaernets Televaesen
Lergravsvej 55
Copenhagen S', Denmark — 1 copy

Mr. F. Lied
Norwegian Defense Research
Establishment
Kjeller, Norway — 1 copy

Ing. CAPT N. Berkay
Seyir Ve HDR D
CUBUKLU
Istanbul, Turkey — 1 copy

National Liaison Officers

Mr. Sv. F. Larsen
Danish Defense Research Board
Østerbrogades Kaserne
Copenhagen Ø, Denmark — 1 copy

CDR R. J. M. Sabatier
EMM/TER
2 Rue Royale
Paris 8e, France — 1 copy

Capitano di Fregata U. Gilli
Stato Maggiore della Marina
Roma, Italia — 1 copy

LCDR J.W. Davis, USN
Office of Naval Research
Branch Office, London
Box 39, Fleet Post Office
New York, N.Y. 09510 — 1 copy

CDR Jose E.E.C. de Ataide
Instituto Hydrografico
Rua Do Arsenal Porta H-1
Lisboa 2, Portugal — 1 copy